AD-A033 136 NAVAL OCEANOGRAPHIC OFFICE WASHINGTON D C MARINE SC--ETC F/G 20/1
AN OCEANOGRAPHIC AND ACOUSTIC STUDY OF A ONE-DEGREE SQUARE IN T--ETC(U)
SEP 65 R E JOHNSON

UNCLASSIFIED N00-IM-0-9-65 NL

| OF |
AD A033136

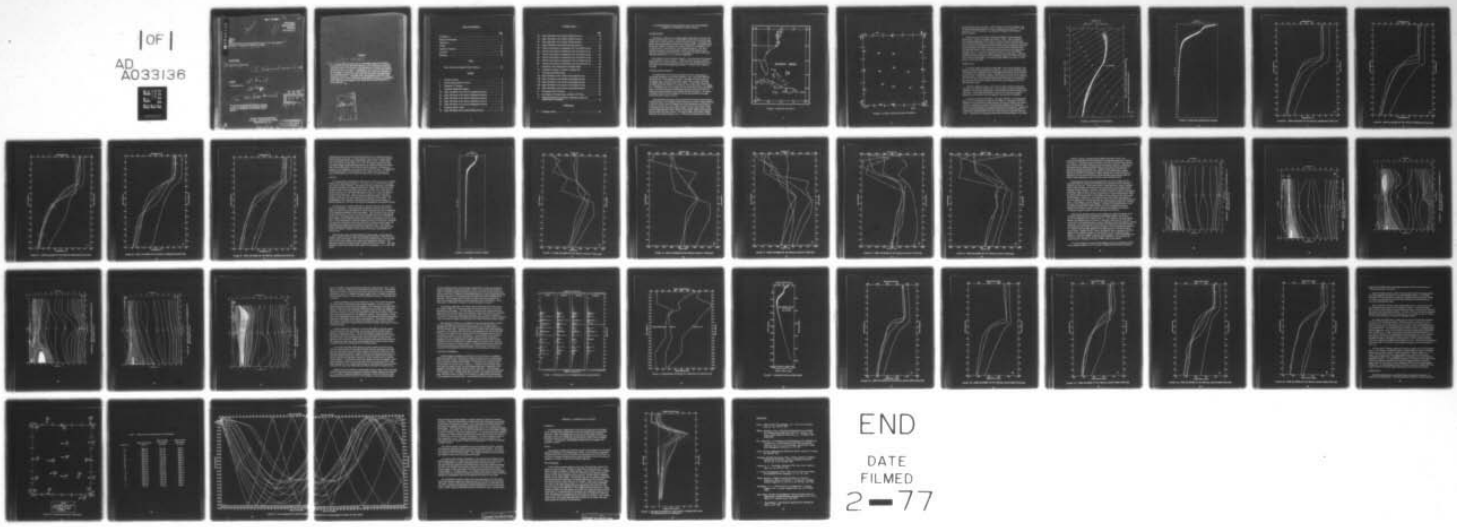

END

DATE FILMED
2-77

MOST Project -2 FG

Good

(1)

INFORMAL MANUSCRIPT REPORT NO. 0-9-65

TITLE

(6) AN OCEANOGRAPHIC AND ACOUSTIC STUDY OF A ONE-DEGREE SQUARE IN THE WESTERN NORTH ATLANTIC.

AUTHOR

(10) ROLAND E. JOHNSON

(9) Informal manuscript repts

DATE

(11) Sep 65

SEPTEMBER 1965

(12) 47p.

(14) NOO-IM-0-9-65

This manuscript has a limited distribution, therefore in citing it in a bibliography, the reference should be followed by the phrase UNPUBLISHED MANUSCRIPT.

MARINE SCIENCES DEPARTMENT
U. S. NAVAL OCEANOGRAPHIC OFFICE
WASHINGTON 25, D.C.

401263

ABSTRACT

(25 Oct - 11 Nov 1963)

An intensive Nansen cast survey of a one-degree square in the Western North Atlantic revealed significant variations in the distribution of properties. A definite pattern of fine structure of the properties was revealed in the upper 500 meters of the water column. Comparison of such a structure with historical BT data suggests the possibility of the Antilles Current being more important in heat exchange processes in the upper strata than the energy exchange through atmospheric interaction. Reduction of the oceanographic model of this one-degree square into acoustic information reveals greater variations in convergence zone ranges and wider changes in zone widths than previously expected in a small ocean area.

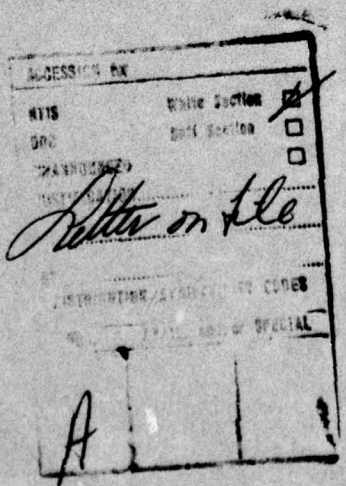

TABLE OF CONTENTS

TABLE

FIGURES

FIGURES (Cont'd)

APPENDIXES

AN OCEANOGRAPHIC AND ACOUSTIC STUDY OF A ONE-DEGREE SQUARE IN THE WESTERN NORTH ATLANTIC

INTRODUCTION

This study is a report of a one-degree square labeled Area B located in the Western North Atlantic Ocean. The USS PREVAIL (AGS-20) collected oceanographic data in Area B during the period 25 October through 11 November 1963. Twenty-three oceanographic Nansen stations were occupied, supplemented by 18 bottom core samples, 4 plankton tows, bottom reflectivity measurements at the 23 stations and 13 tracks underway, and 76 bathythermograms. This report presents an analysis of the serial stations and BT's with the emphasis placed upon the actual measured quantities (i.e. temperature and salinity) rather than computed properties (i.e., σ_t or dynamic topography).

The location of Area B is shown in Figure 1, and the location of the oceanographic stations is shown in Figure 2. The stations retain the same numerical designation as was originally planned for the cruise even though the actual transects were run north-south beginning at Station 1. Stations 4 and 7 were not occupied.

PHYSICAL OCEANOGRAPHY

An understanding of the physical properties of Area B is best gained by considering the regional factors which influence, alter, and locally determine the distribution of oceanographic variables. Northeast of the study area lies the Sargasso Sea, an area relatively free of major ocean currents, and having the highest surface salinities in the North Atlantic. Schott (1942) reports that salinities greater than 36.00 $^{o}/_{oo}$ are found to at least 400 meters in the Sargasso Sea. Immediately south of the Sargasso Sea lies the Antilles Current, the northern branch of the North Equatorial Current which transports saline water from the Sargasso towards the junction of the Antilles with the Gulf Stream. This current is thought to exert the major influence in altering the properties of the upper strata of the water column in Area B.

From the surface downwards, the gross features of the water structure may be characterized as: local isothermal surface water which overlies a salinity maximum; a relatively uniform region of Sargasso water whose temperature and salinity are relatively invariant over a small range of values; North Atlantic Central Water, a well-defined water mass whose upper boundary includes Sargasso Water; North Atlantic Deep and Bottom Water, whose cold but slightly fresher waters dominate the lower half of the water column. The limits for these water masses are those defined by the Oceans (Sverdrup, et al., 1942) which designates North Atlantic

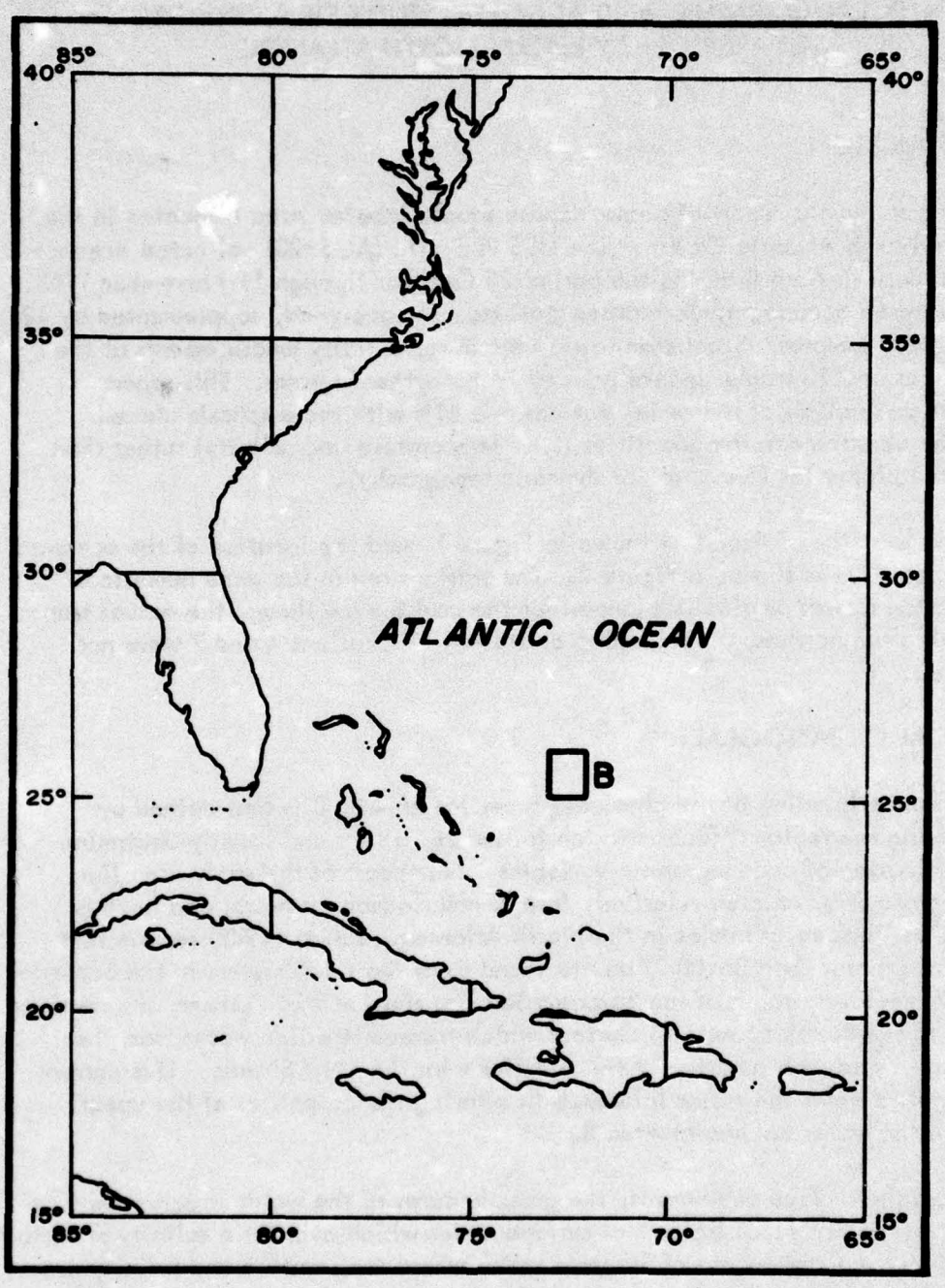

FIGURE 1 LOCATION OF AREA B

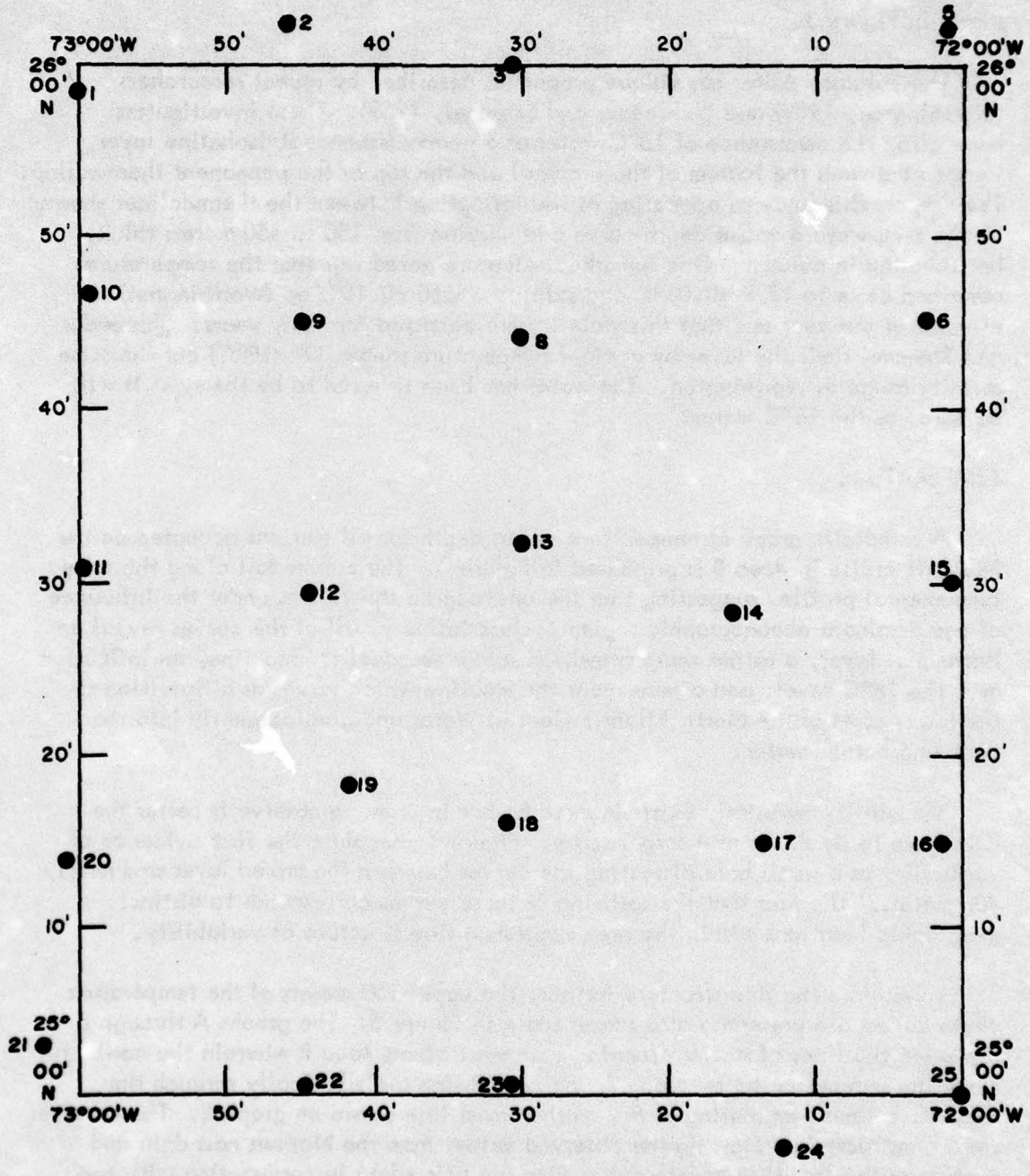

FIGURE 2 STATION LOCATION CHART FOR AREA B

Central Water as lying between 8° - 19°C and 35.10 - 36.70°/oo salinity, and the North Atlantic Deep and Bottom Water as defined by the range 3.5° - 2.2°C and 34.90 - 34.97°/oo salinity. A composite T-S diagram of all stations is shown in Figure 3.

The Sargasso Water has unique properties described by recent researchers (Worthington, 1959) and (Schroeder and Stommel, 1959). These investigators have cited the persistence of 18°C water as a nearly isothermal-isohaline layer located between the bottom of the seasonal and the top of the permanent thermocline. They report this layer as appearing at the inflection between the thermoclines shown by the temperature versus depth curve and varying from 150 to 450 meters thick, but thinning in autumn. One remarkable feature noted was that the temperature remained close to 17.9 ±0.03°C and salinity 36.50 ±0.10°/oo (Worthington) throughout the year and that this stability has persisted for many years. Schroeder and Stommel limit the layer by a wider temperature range (17°-19°C) but the same salinity range as Worthington. The water has been referred to by them, as it will be here, as the 18°C water.

TEMPERATURE

A composite graph of temperature versus depth for all stations occupied on the PREVAIL cruise in Area B is presented in Figure 4. The curves fall along the same fundamental profile, suggesting that the one-degree square was under the influence of one dominant oceanographic regime. Descriptively, all of the curves reveal an isothermal layer, a rather sharp transition into a seasonal thermocline, an inflection near the 18°C level, and a permanent thermocline which serves as a transition to the lower parts of the North Atlantic Central Water and grading gently into the deep and bottom water.

Variability definitely exists in Area B, but in order to observe it better the data have to be shown at a larger scale. Figure 4 does show the first evidence of variability as a small hole dissecting the curves between the mixed layer and nearly 400 meters. The fact that the splitting of these curves corresponds to distinct geographic locations within the area suggests a fine structure of variability.

To explore the fine structure further, the upper 150 meters of the temperature depth curves are presented at a larger scale in Figure 5. The graphs A through E represent the lines of stations running east-west across Area B wherein the northernmost line is represented by graph A and progressing alphabetically through the successive lines terminating at the southernmost line shown on graph E. These curves were constructed by plotting the observed values from the Nansen cast data and modifying the resulting smooth curve with the BT's taken in conjunction with each station. Examination of these graphs reveals that the splitting begins at the surface

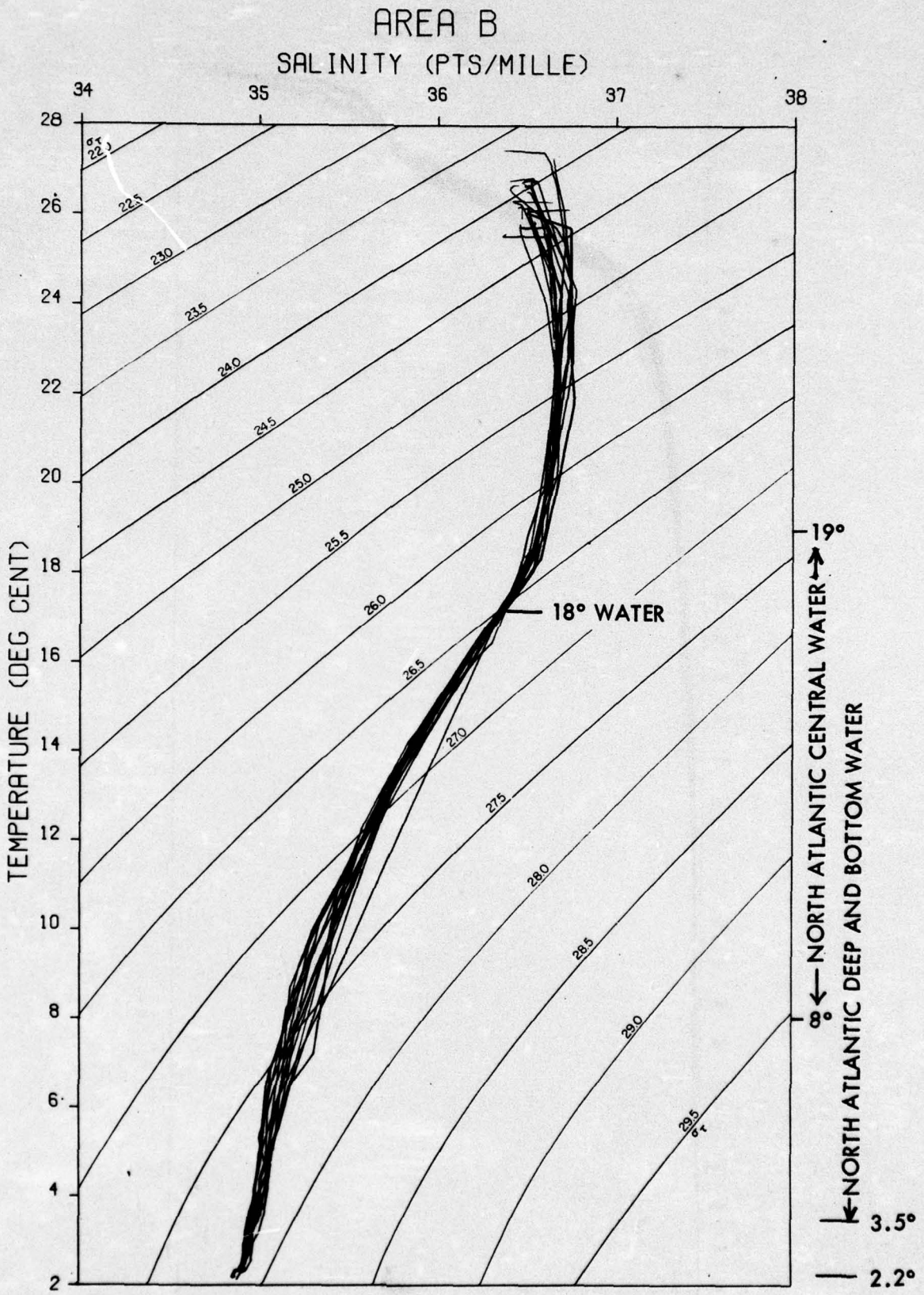

FIGURE 3 COMPOSITE T/S DIAGRAM

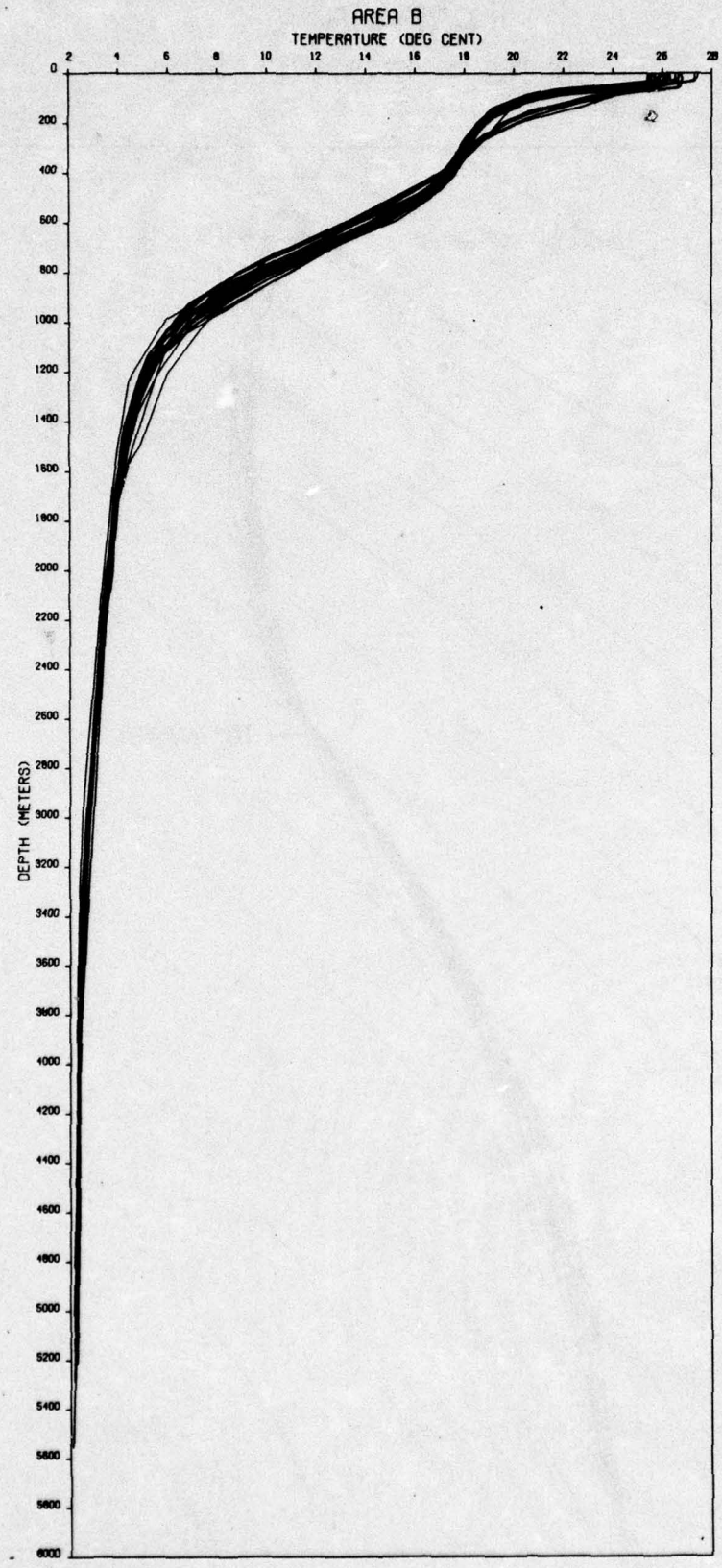

FIGURE 4 COMPOSITE TEMPERATURE DIAGRAM

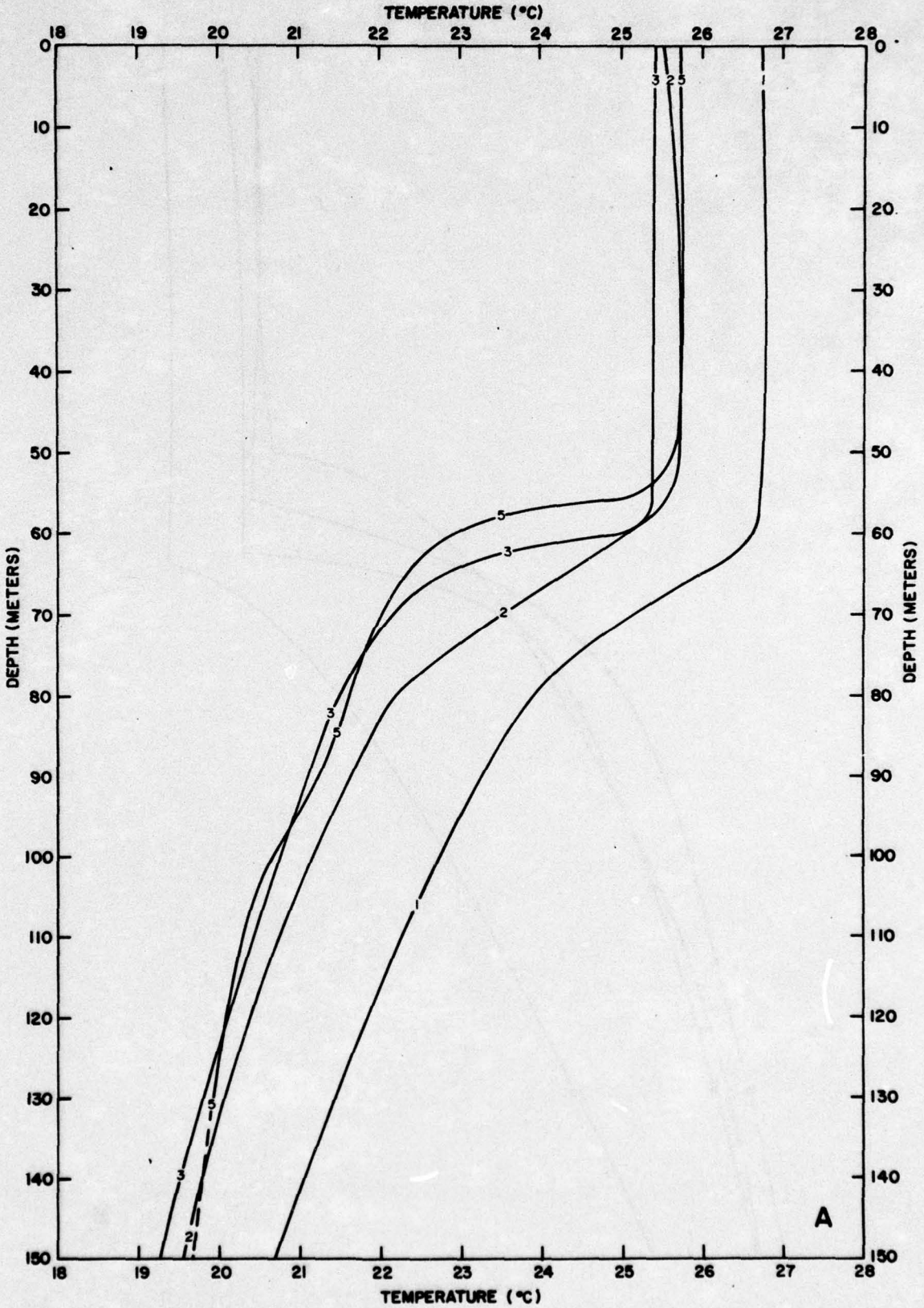

FIGURE 5A UPPER 150 METERS OF THE VERTICAL TEMPERATURE STRUCTURE

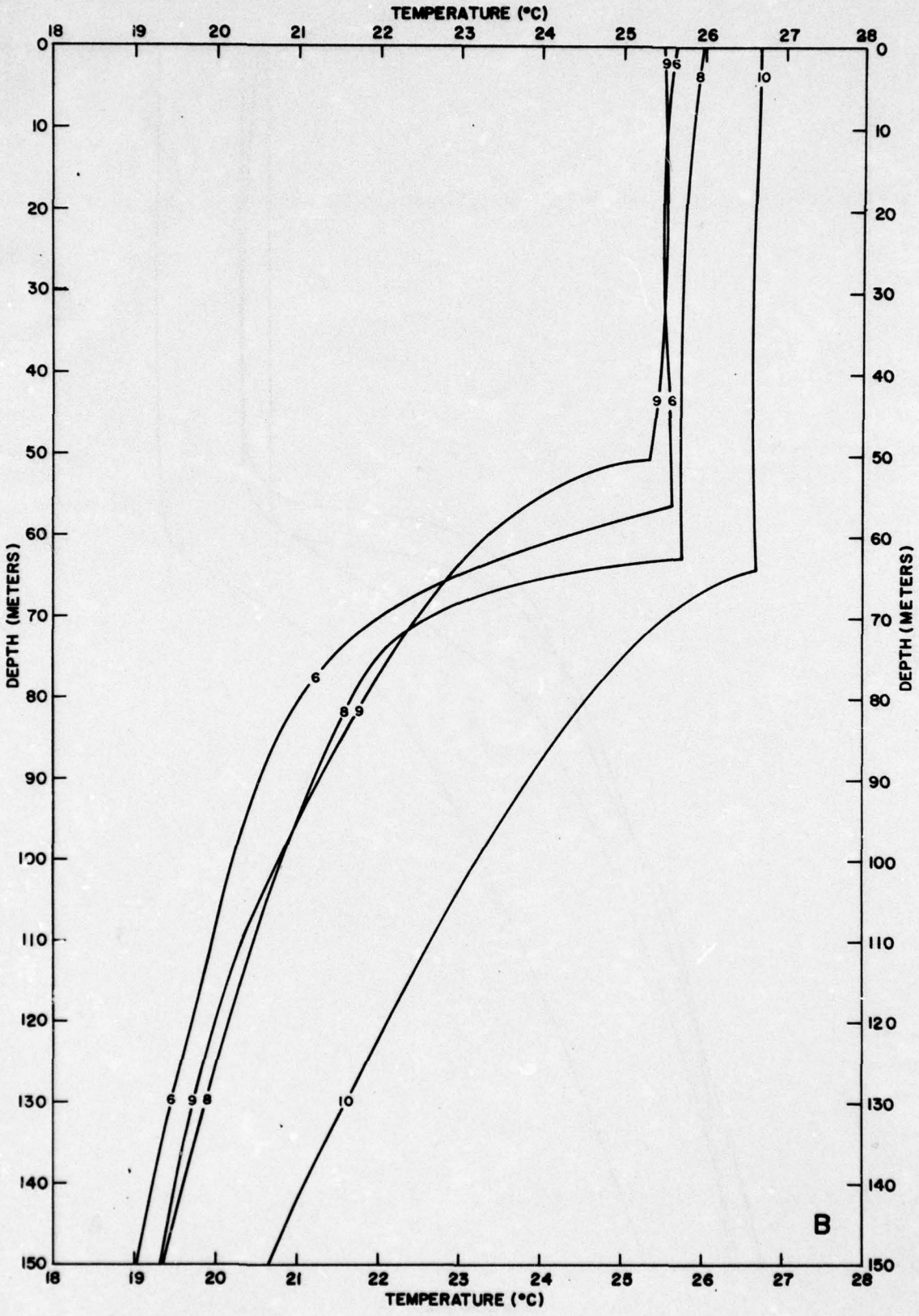

FIGURE 5B UPPER 150 METERS OF THE VERTICAL TEMPERATURE STRUCTURE

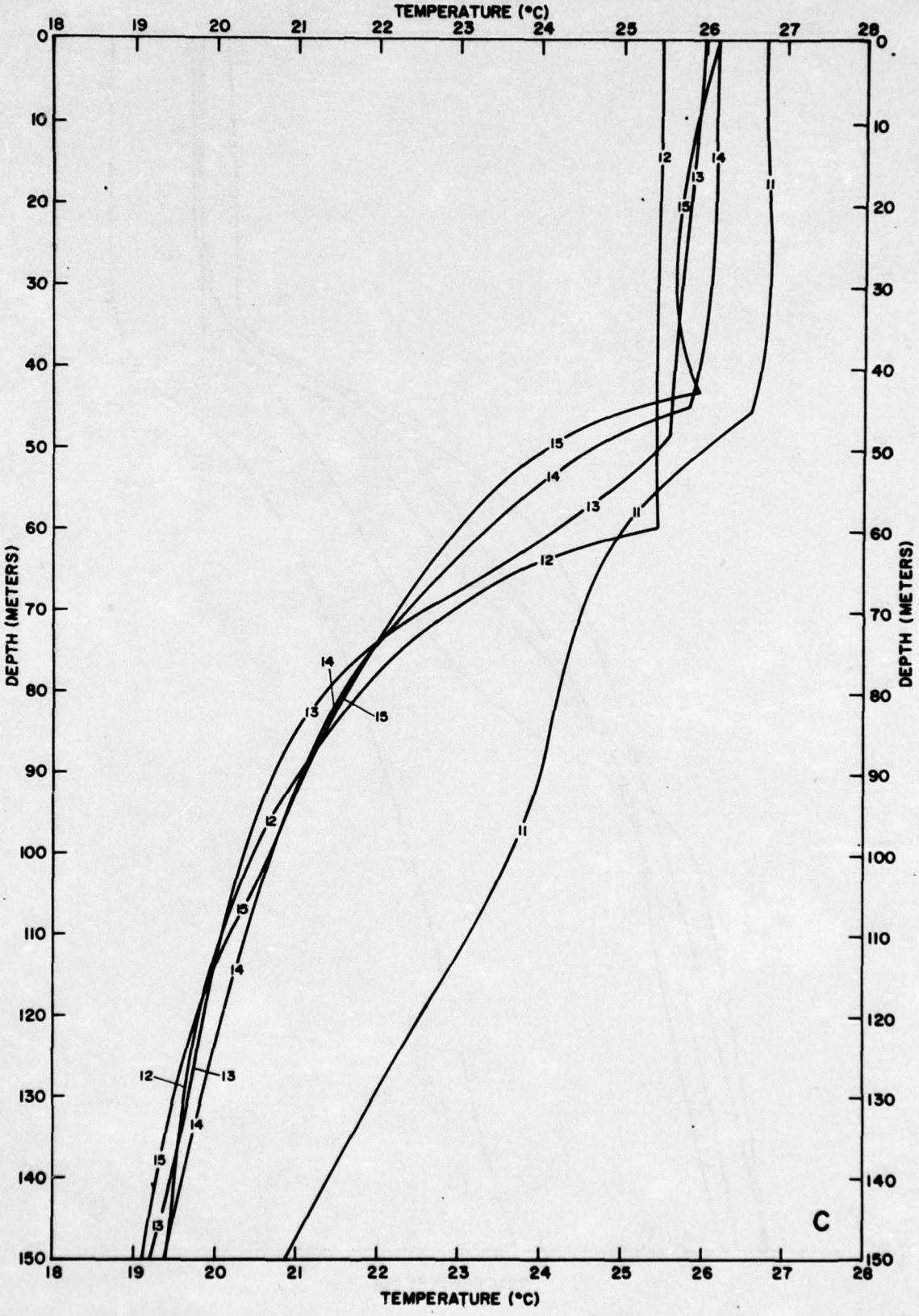

FIGURE 5C UPPER 150 METERS OF THE VERTICAL TEMPERATURE STRUCTURE

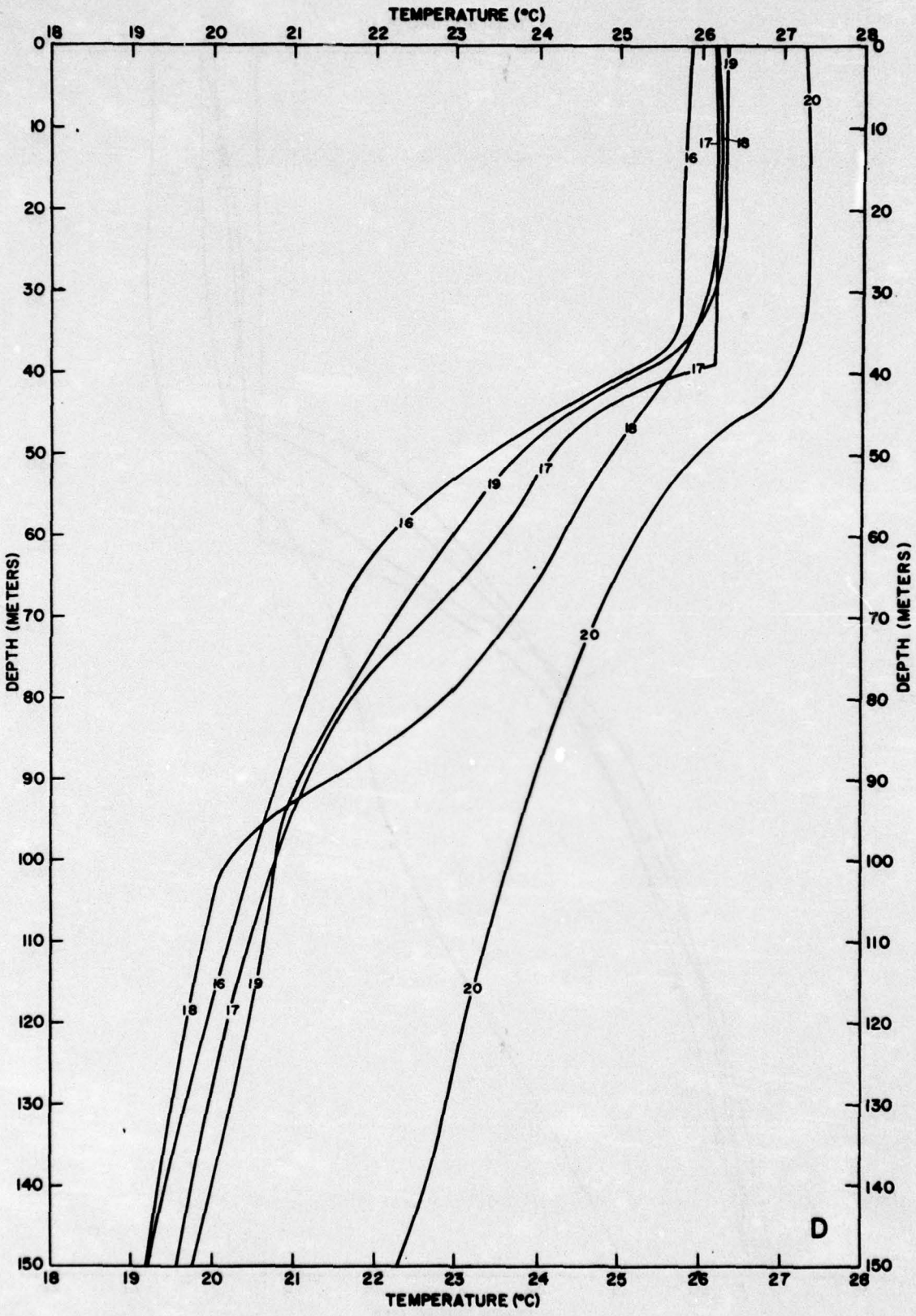

FIGURE 5D UPPER 150 METERS OF THE VERTICAL TEMPERATURE STRUCTURE

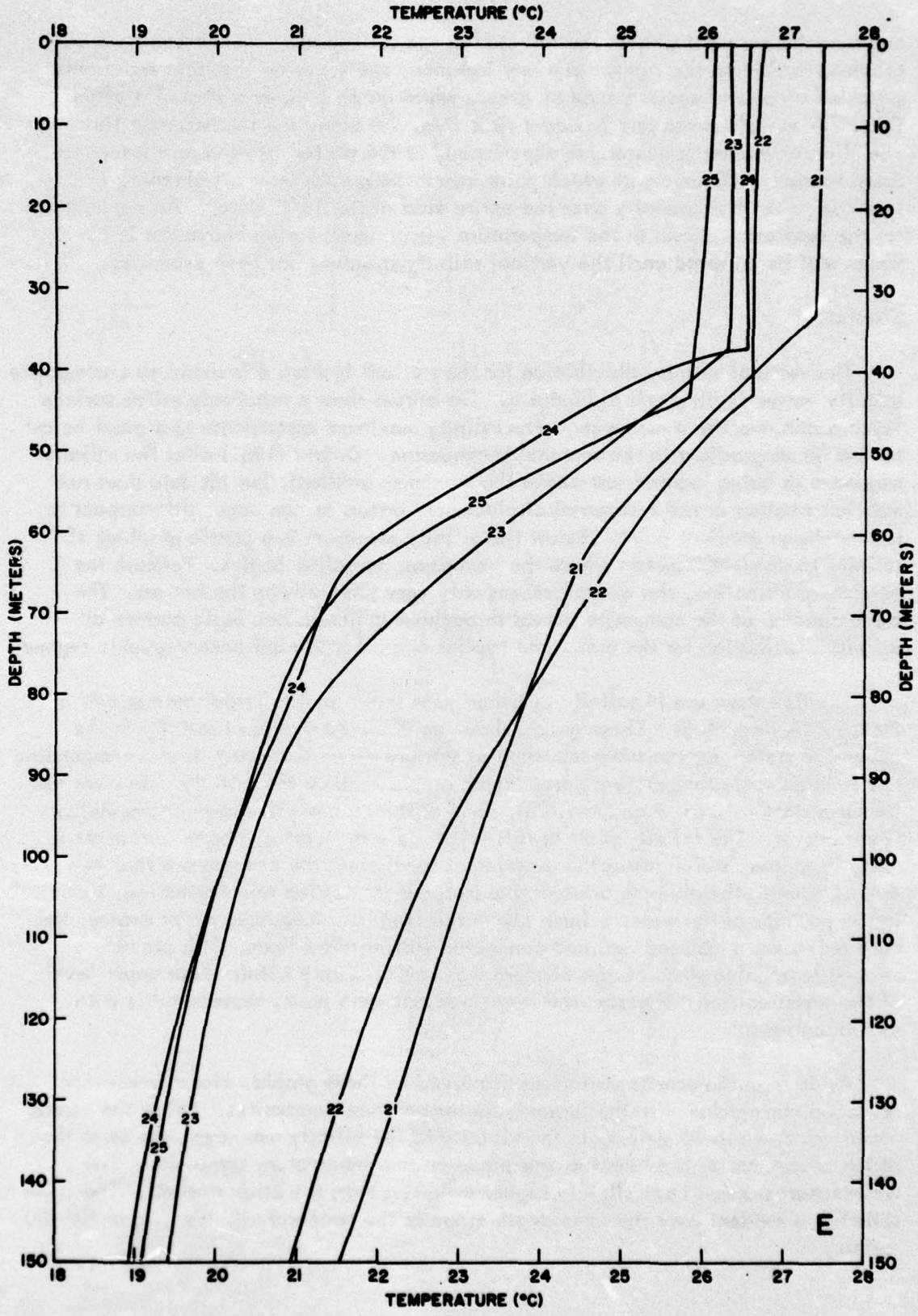

FIGURE 5E UPPER 150 METERS OF THE VERTICAL TEMPERATURE STRUCTURE

and that the curves bunch on the left side of the split so as to isolate one (two on graph E) station on the right. In every instance, the curve on the right represents a station along the western edge of Area B while graph E shows a western station (No. 21) as well as the one adjacent to it (No. 22) along the southernmost line. The slightly warmer temperatures experienced at the western stations are traceable down to about 400 meters at which point composite graphs show a tightening in response to the homogeneity over the entire area of the 18°C water. An explanation for the separation shown in the temperature versus depth curves above the 18°C water will be deferred until the vertical salinity structure has been examined.

SALINITY

The vertical salinity distribution for the stations in Area B is shown as a composite salinity versus depth graph in Figure 6. The curves show a relatively saline surface layer which overlies a maximum. The salinity maximum corresponds to a point below the maximum gradient in the seasonal thermocline. Defant (1961) cites the salinity maximum as being located just above the maximum gradient, but his data does not mention whether or not a seasonal displacement occurs or can occur with respect to the maximum gradient point. Below the salinity maximum is a gentle gradient of salinity to about 400 meters where the permanent halocline begins. Beneath the permanent halocline, the water freshens only very gradually to the bottom. The close-spacing of the composite curves throughout indicates one basic pattern of salinity distribution for the area, and implies one preponderant oceanographic regime.

The fine structure in salinity distribution is shown by the large scale graphs in Figure 7 (A through E). These graphs show the observed values of salinity in the upper 150 meters for the same sequence of stations along east-west lines corresponding to the large scale temperature versus depth graphs. Since the salinity data were lost for some stations (No. 9 and No. 23), some of the graphs will show correspondingly fewer curves. The salinity plots at this large scale show rather abrupt variations in many instances, which raises the question as to whether the changes are real or merely errors. Due to the absence of objective methods for making this distinction, especially in the portions of the water column above the level of recognized water masses, the data points were assumed real and connected with straight lines. This procedure seemed reasonable since abrupt changes were evident only within these upper levels of the water column, whereas, the lower portions were easily representable with smooth curves.

Aside from the erratic variations displayed by these graphs, closer inspection reveals a correlation with the large-scale temperature composites. Below the erratic variations down to 60 meters, in the vicinity of the salinity maximum, the same separation of the curves is evident as was noted on the temperature composite. The westernmost stations have slightly higher salinities than the other stations. The curve-splitting is evident over the same depth range as the temperature, i.e., to about 400 meters.

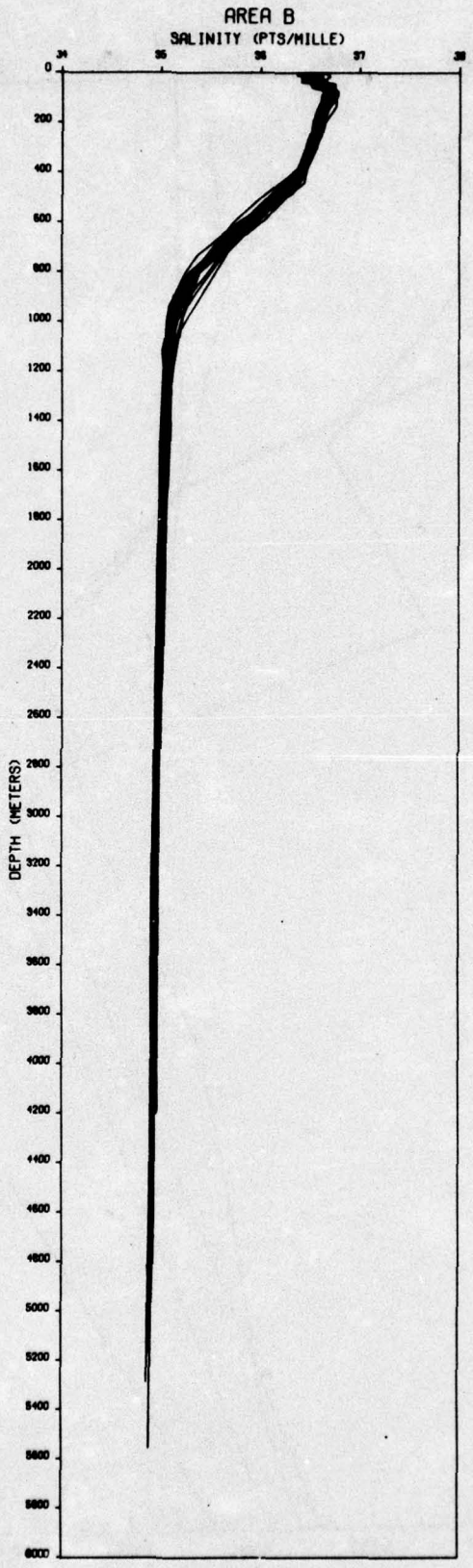

FIGURE 6 COMPOSITE SALINITY GRAPH

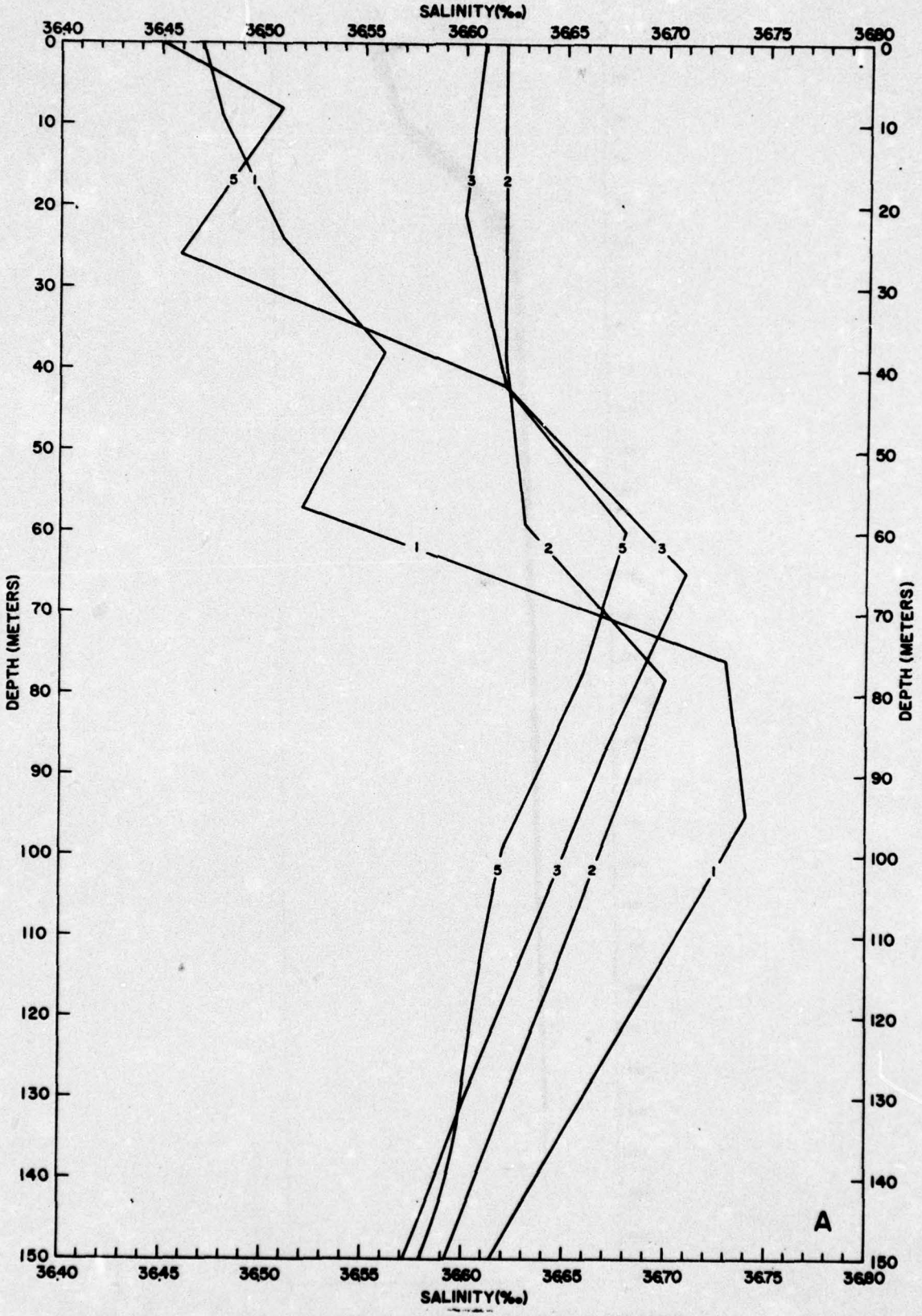

FIGURE 7A UPPER 150 METERS OF THE VERTICAL SALINITY STRUCTURE

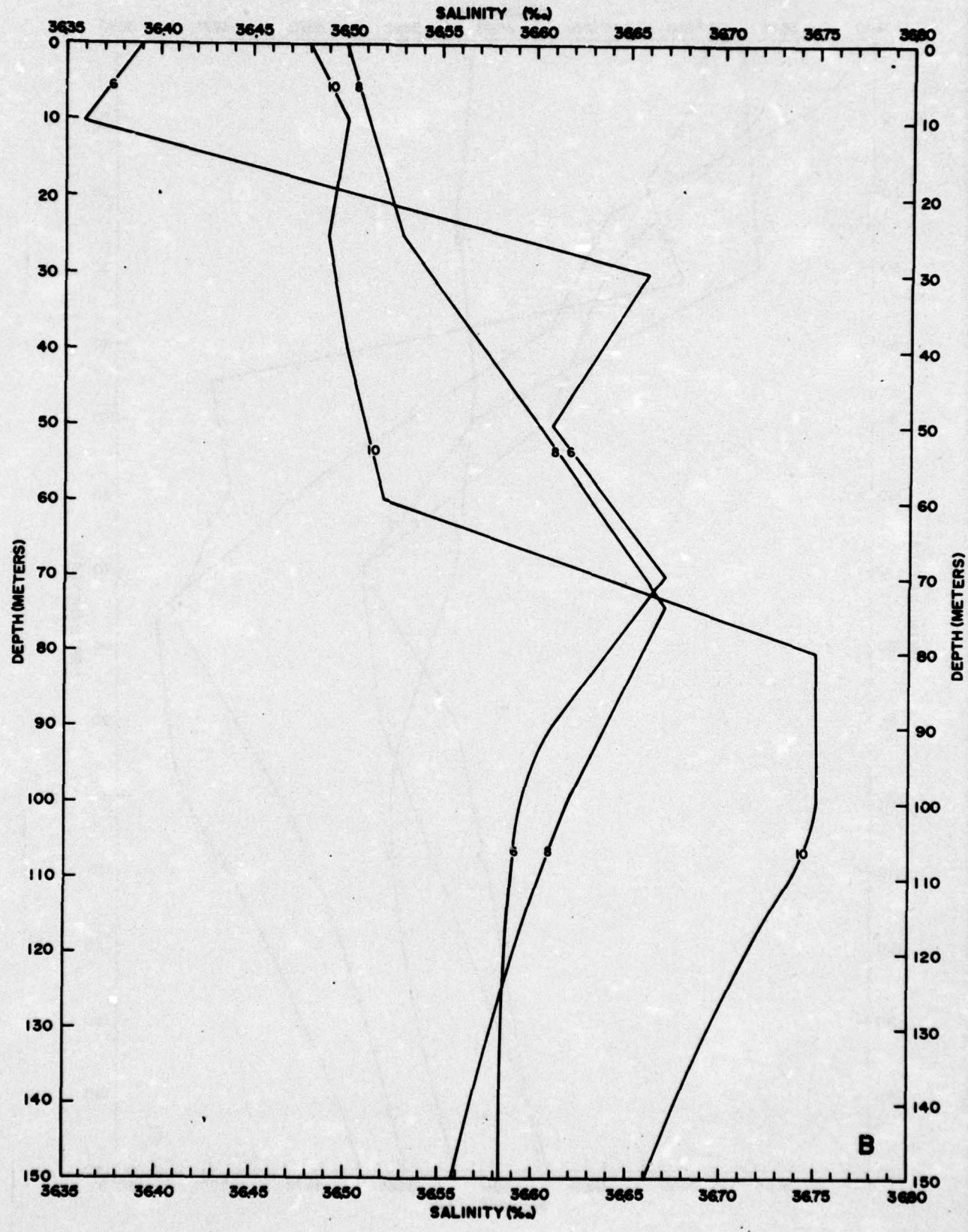

FIGURE 7B UPPER 150 METERS OF THE VERTICAL SALINITY STRUCTURE

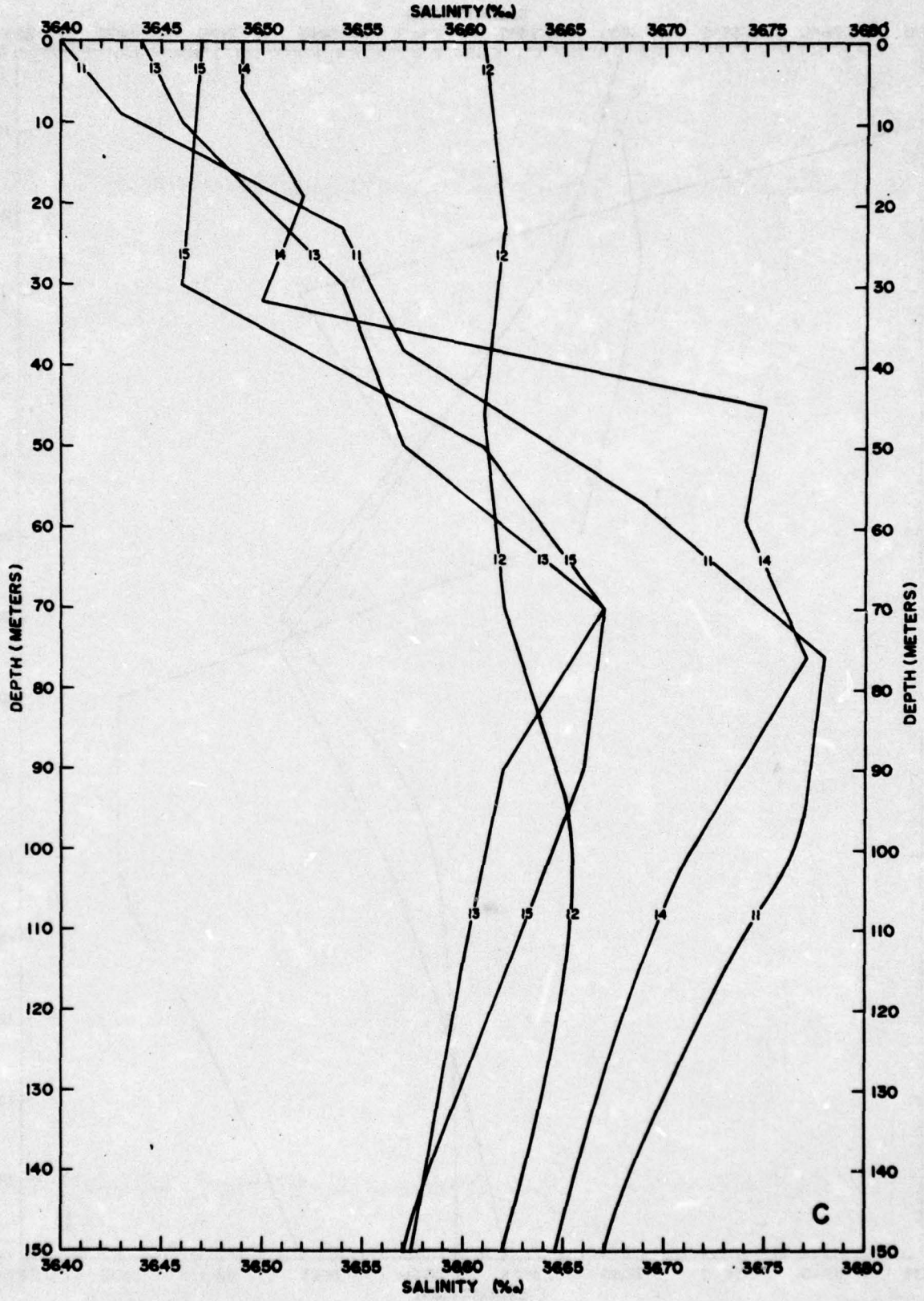

FIGURE 7C UPPER 150 METERS OF THE VERTICAL SALINITY STRUCTURE

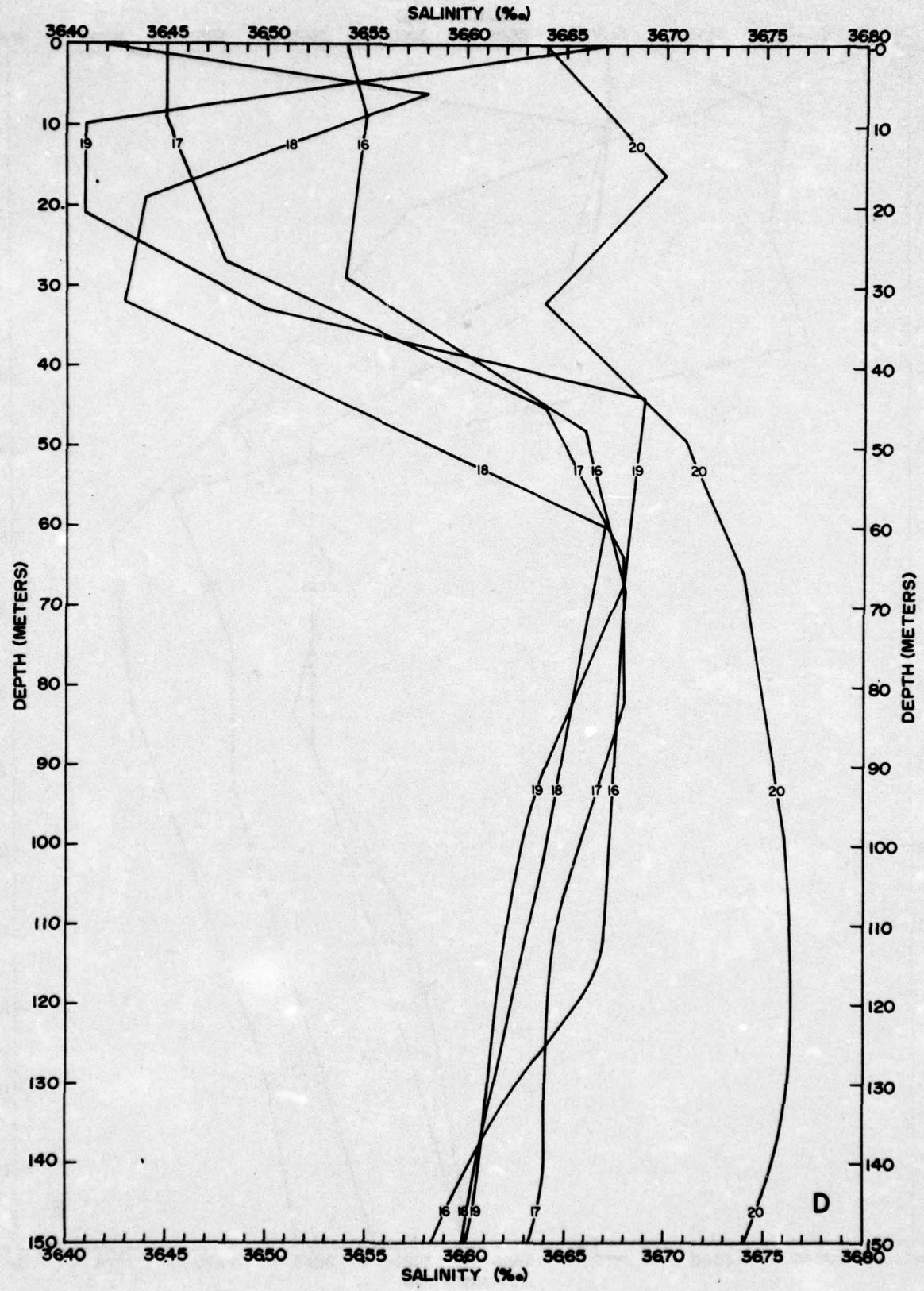

FIGURE 7D UPPER 150 METERS OF THE VERTICAL SALINITY STRUCTURE

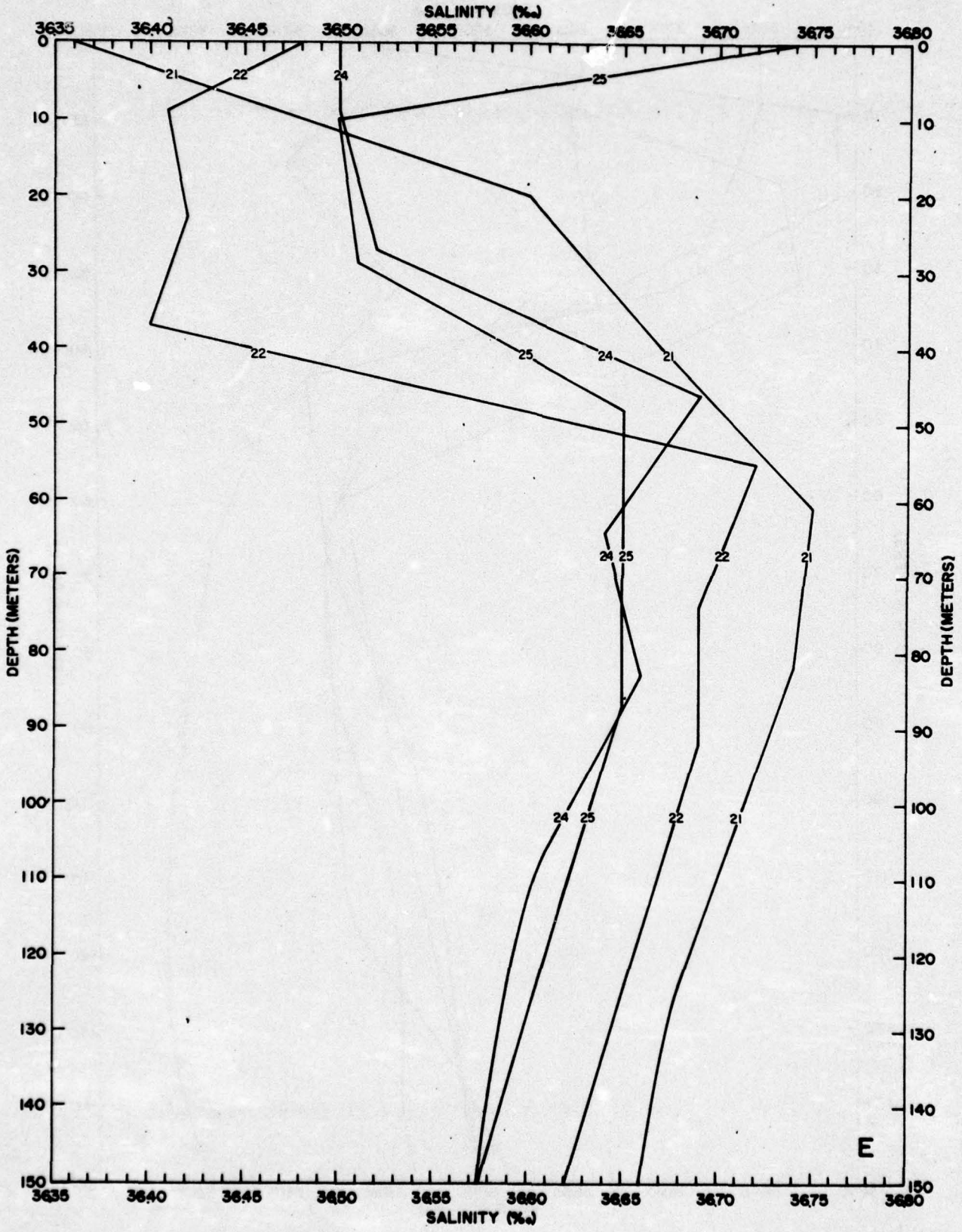

FIGURE 7E UPPER 150 METERS OF THE VERTICAL SALINITY STRUCTURE

A series of vertical cross-sections have been constructed to show a two-dimensional representation of the distribution of the measured properties in Figure 8 (A through F). The graphs represent the series of 5 lines of stations running west-east across the area (A through E) and one section running north-south (F). Contoured on these graphs are the observed salinities shown by solid lines with the observed temperatures superimposed as dashed lines. Shading is based upon salinity values wherein the densest shading shows the salinity maximum defined here as banded between the 36.60°/oo isohalines; the lighter shading below 36.40°/oo shows the beginning of the permanent halocline, and the unshaded region between these two salinity values indicates the zone of the 18°C water mentioned earlier.

This presentation shows many interesting features as well as exhibits why the composites showed the splitting effect between the westernmost and the remainder of the stations in the area. Shown quite clearly in these sections is a layer of maximum salinity water stretching across the entire area, but having a core of higher salinity along the western boundary. Moreover, the isotherms are seen to depress westward indicating a region of warmer water at every depth to which the saline core corresponds. It should be noted that this core of warm saline water is located almost entirely within the seasonal thermocline which is well-defined in these sections by the close spacing of the isotherms. Station No. 14 on graph C shows a lens of warm saline water of the same magnitude as the maximum core, and located within the same salinity maximum layer. In the diagram, it stands apart from the other apparently larger mass, although numerous other interpretations are possible. Certainly it correlates with the core on the western boundary both in terms of salinity as well as temperature structure. Another lens is evident in graph D where a lens of lower salinity water is shown overlying the salinity maximum layer and extending to the surface.

Aside from the lenticular features, the unshaded zone depicts the domain of the 18°C water which extends over the entire area bounded locally by the 36.60 to 36.40°/oo isohalines in the vicinity of the 17° - 19°C isotherms. The wide spacing between the isopleths portray this zone as a relatively uniform section of the water column which, as the diagram shows, varies in thickness over the area generally thinning westwardly. This uniform property of the 18°C water makes this zone worthy of separate distinction even though, as previously defined, it lies for the most part below the 19° isotherm which has been specified as the upper boundary of the North Atlantic Central Water. Beneath the 18°C water, the transition into the permanent halocline begins and the flattening tendency for the isotherms as well as isohalines begins. Graph F, a north-south diagram along the western boundary, gives the impression that the layer of maximum salinity, though varying in thickness is also thinning to the north and south. Thinning of the layer of 18°C water is also evident.

It is now of interest to account for the presence of the layer of maximum salinity and to ascertain whether or not it is merely a transient feature observed during the

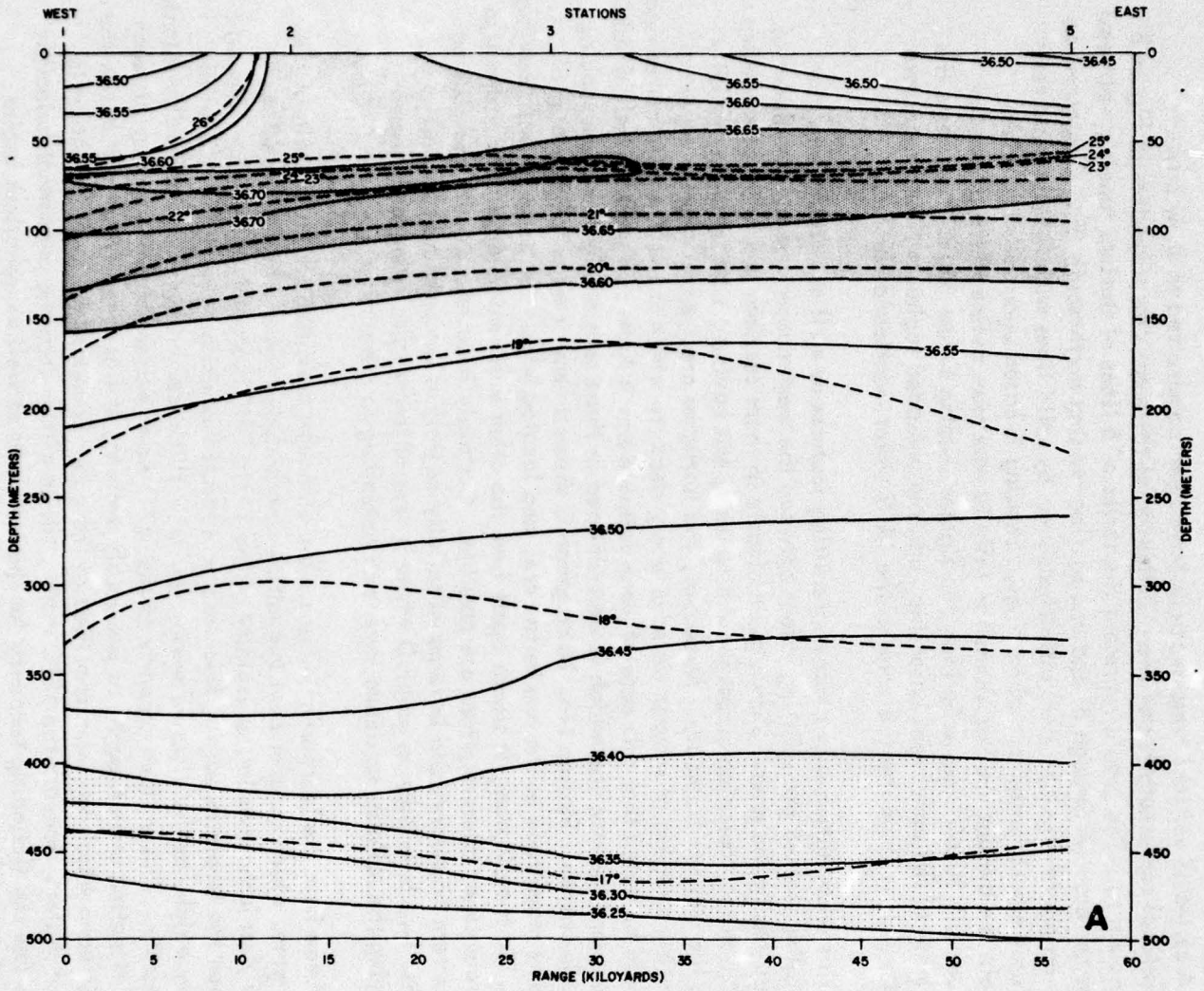

FIGURE 8A VERTICAL CROSS SECTION OF TEMPERATURE (°C) AND SALINITY (o/oo)

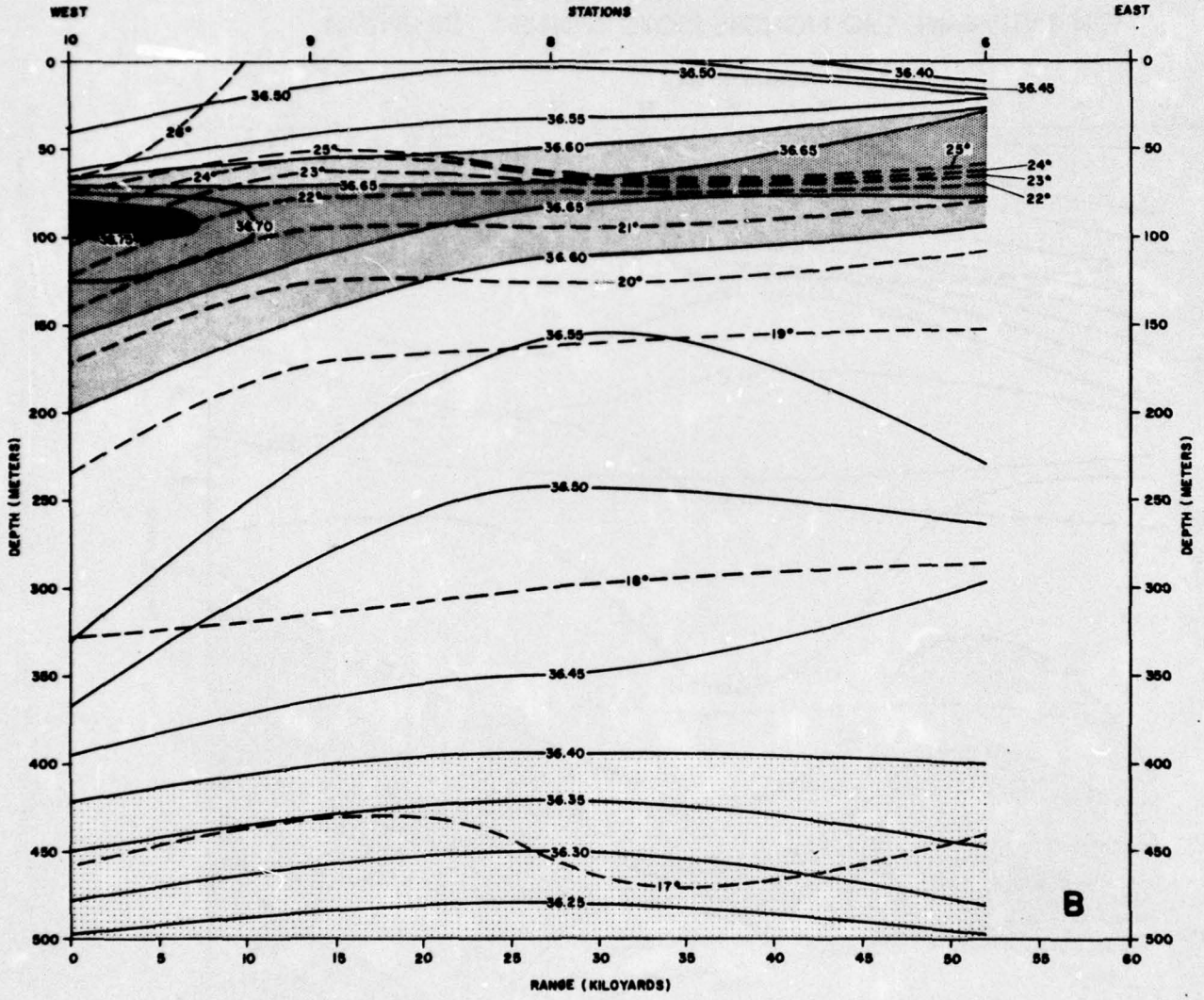

FIGURE 8B VERTICAL CROSS SECTION OF TEMPERATURE (°C) AND SALINITY (o/oo)

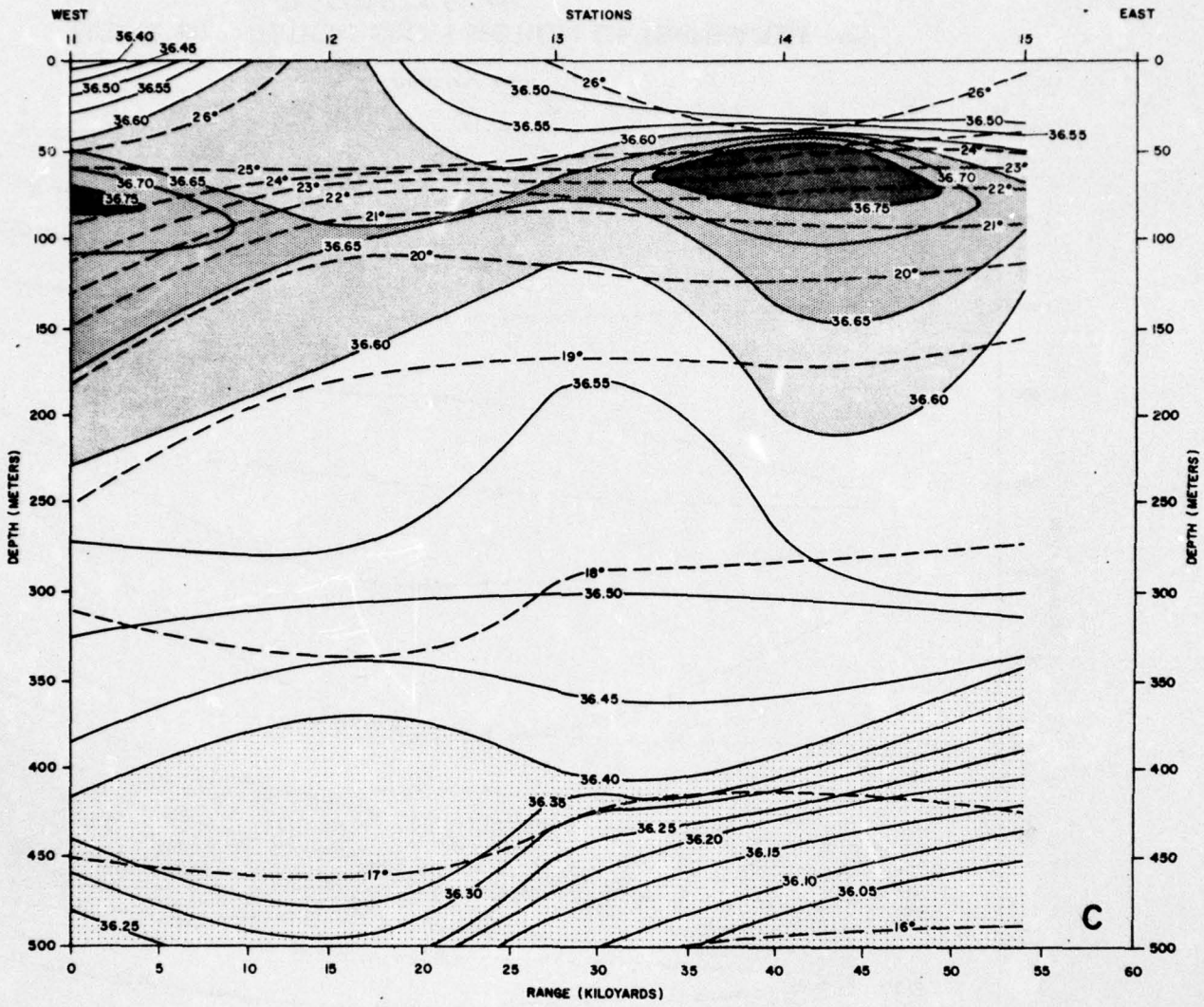

FIGURE 8C VERTICAL CROSS SECTION OF TEMPERATURE (°C) AND SALINITY (o/oo)

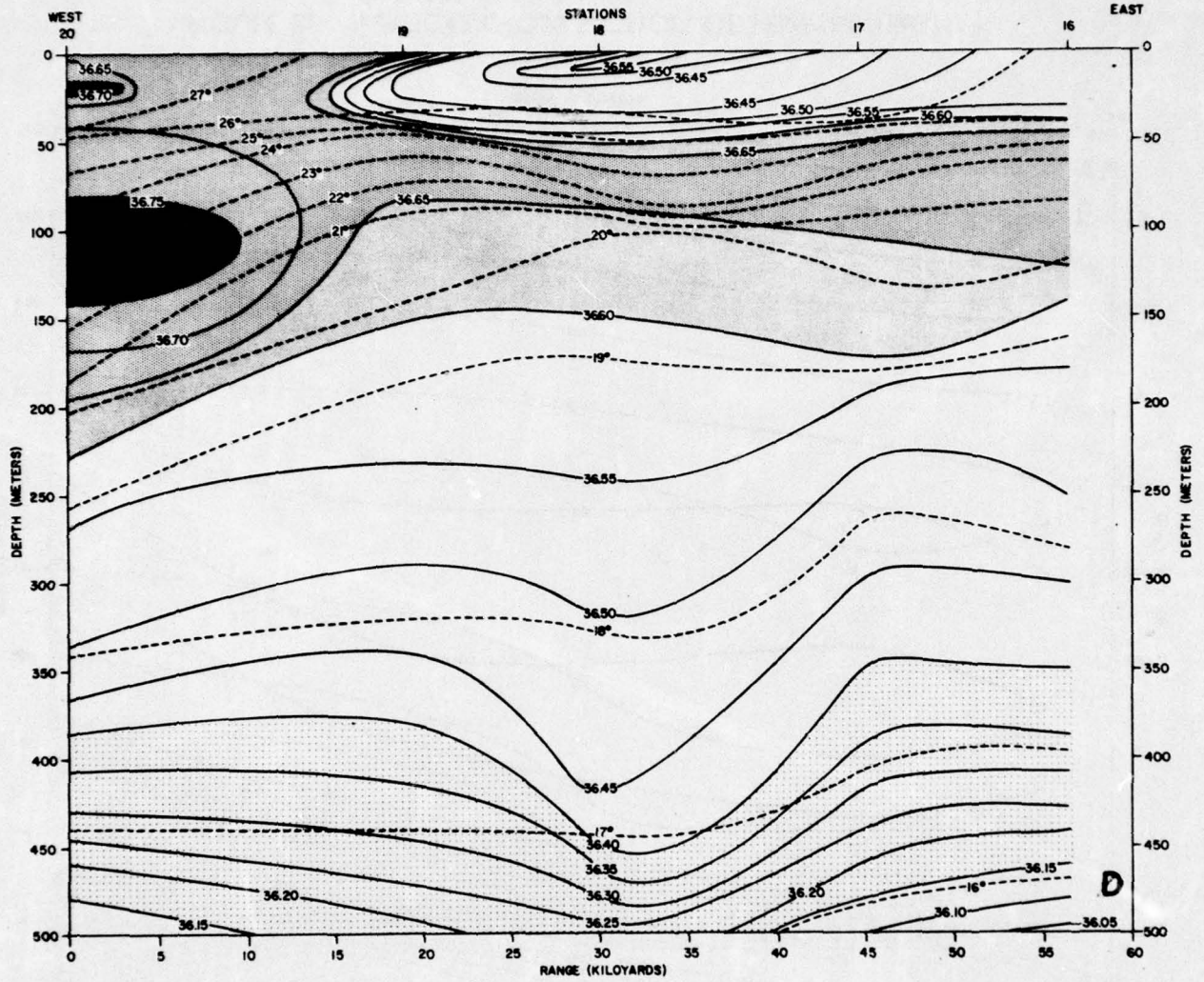

FIGURE 8D VERTICAL CROSS SECTION OF TEMPERATURE (°C) AND SALINITY (o/oo)

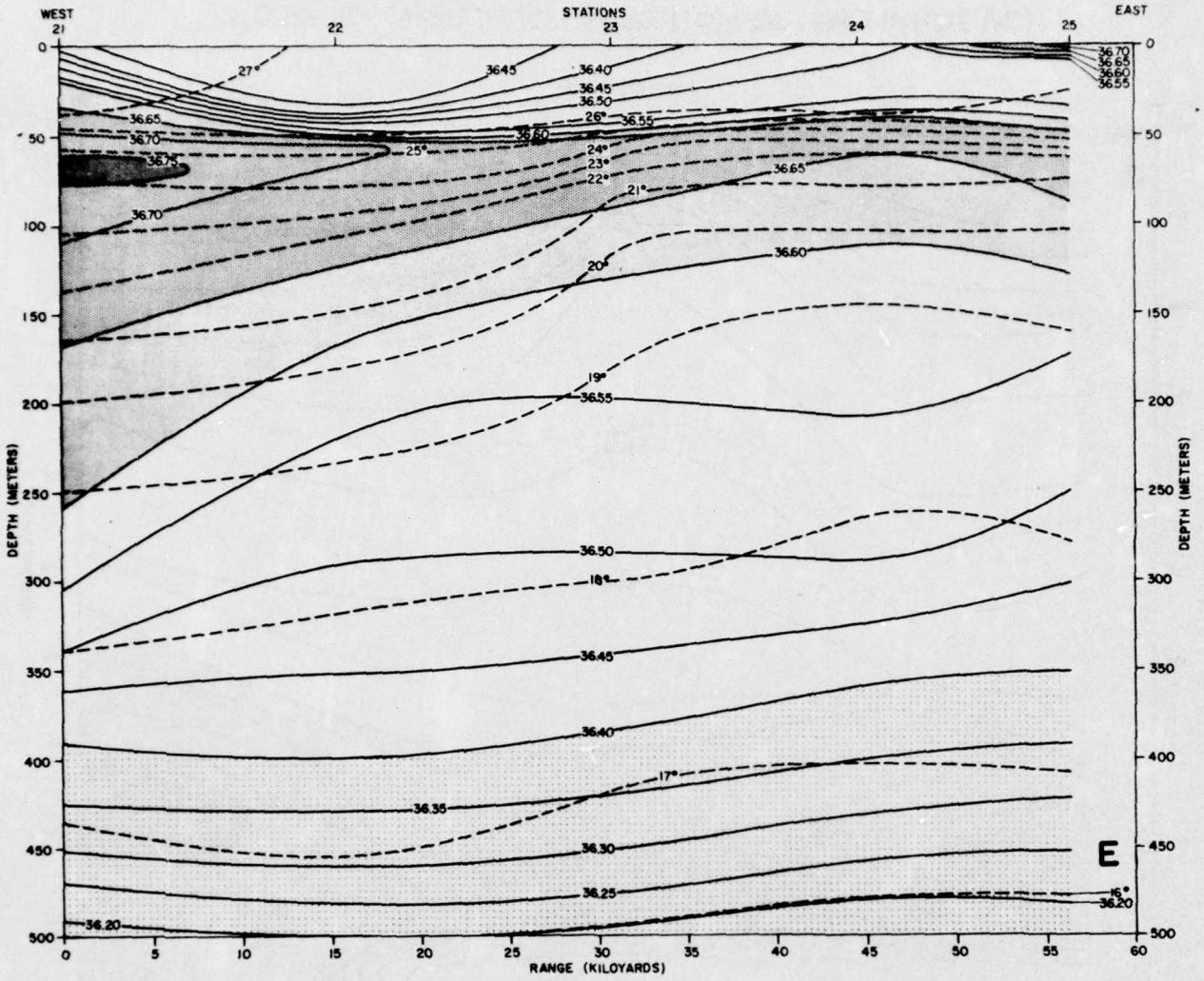

FIGURE 8E VERTICAL CROSS SECTION OF TEMPERATURE (°C) AND SALINITY (o/oo)

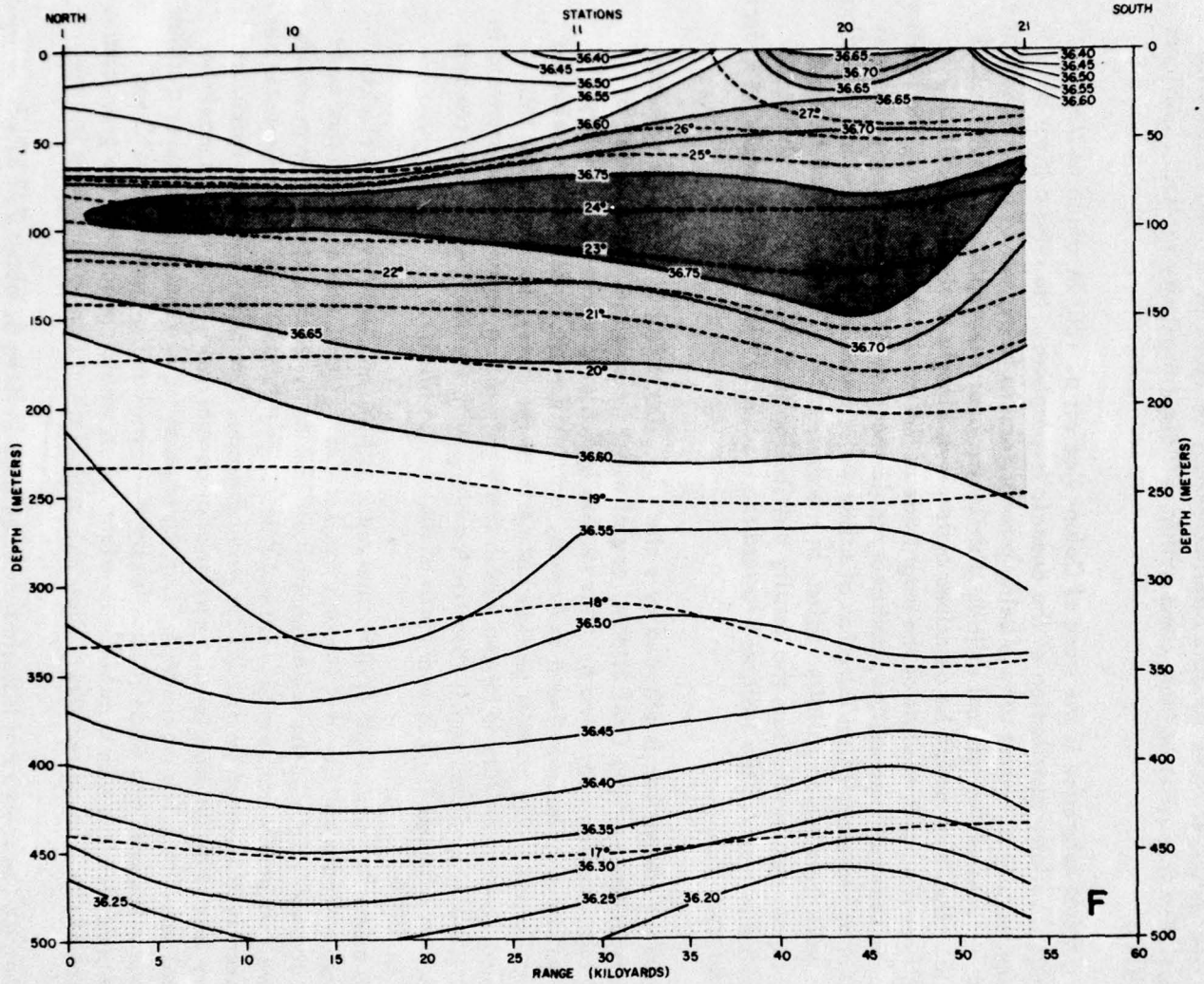

FIGURE 8F VERTICAL CROSS SECTION OF TEMPERATURE (°C) AND SALINITY (o/oo)

survey, or whether it may be expected to persist for a longer period of time. In this regard, comparisons of PREVAIL data with historical data were made. Unfortunately, the sparsity of historical Nansen cast data within Area B will not permit an adequate comparison; however, a reasonable alternative may be found in regional studies which have included this area, or have come within sufficient proximity to yield significant correlation.

A general reference is the work of Defant (loc cit p. 166) in which he discusses the vertical salinity distribution of the oceanic troposphere. He cites a layer of maximum salinity as almost always being present, and as being one of the most characteristic features of the vertical salinity distribution over the tropical and subtropical Atlantic. The layer which he describes corresponds closely to the one exhibited in Area B from the point of view of the magnitude of the maximum of salinity, the position within the seasonal thermocline, and geographic location. Correspondingly, he sees this layer as representing an intrusion of saline water beneath the surface and spreading equatorward from higher salinity regions in the subtropics. This southward transport would appear reasonable from the density distribution (not shown) which, similar to the downward trend of the isotherms toward the western stations, would imply an overall transport southward.

Another comparison is afforded by a study by Wüst (1930) in which he presents 6 cross-sections over the Gulf Stream, one of which crosses the Florida Strait at Bimini to a location near Area B. This section indicates a maximum of salinity of the identical magnitude as found in Area B, which Wüst associates directly with the Antilles Current. On another section just north of the latter, he shows that this maximum layer of salinity is formed within the highly saline water further eastward in the Sargasso Sea, sinks, and is then carried along with the Antilles Current towards its junction with the Gulf Stream north of the Florida Straits.

In an earlier work Wüst (1924) observed 2 salinity maxima east of the Florida Current, traced a portion of it through the Antilles Current, and observed that both had a common origin in the saline central portions of the North Atlantic from which they were laterally transported. Lateral transfer of this same type of saline water has also been substantiated by Parr (1936) who concludes that along with this maximum salinity layer may be associated a maximum of current velocity as well as maximum vertical stability. The maximum salinity layer observed in Area B is probably a rather permanent feature, and since it has also been shown that the stratum of 18°C water which underlies it is also a rather stable feature, it would appear that the gross characteristics of this area do not likely show any radical alterations of structure in time.

Despite the sparsity of historical Nansen data in Area B, about 732 BT's have been taken by various ships within the area and in the 8 one-degree squares which surround it. In an effort to compare the PREVAIL cruise data in Area B with historical data, temperatures were read from these BT's for all months at a series of selected depths.

At each preselected depth, the total range of temperature variation was recorded by plotting a distribution made up of intervals 1/10°F in size over the entire observed range. To eliminate possibly faulty data or extreme values which occur less than one per cent of the time, a criterion was established wherein any single isolated observation which fell more than 1°F from the assumed end points of the central distribution was discarded. This procedure resulted in only one observation being rejected at any given level except at 250 meters, where two extreme valves were rejected. A plot showing such a distribution is shown for the first four depths in Figure 9.

The resulting comparison of the Nansen cast with the historical BT data is shown on a graph in Figure 10. These curves give an idea of the total range of variation encountered at each depth. The wider range of variation shown by the historical BT data is due to the fact that these curves represent a total annual variation as contrasted with the Nansen cast data representing only autumn 1962. Despite this imbalance in the data, it can be seen on this graph that both temperature curves achieve a maximum value of variation at roughly the same levels as the layer of maximum salinity is found.

Referring again to Figure 10, an additional scale representing salinity variations has been superimposed to accommodate the curve which, for the depth shown, represents the total range of salinity values (maximum minus minimum) observed in the Area B Nansen casts. Comparison of the 3 curves leads to some rather interesting conclusions. For example, both the Nansen cast temperature data and the historical BT data in Area B show that the maximum variation in temperature does not occur at the surface, but rather in a layer well below it. The coincidence of this maximum variation level with the salinity maximum layer defines the major alterations in temperature structure brought about via lateral exchange with the Antilles Current. The salinity curve in the figure has its highest range at the surface with a secondary maximum in the region of current transport. This indicates that the major alterations of the salinity structure are brought about due to interactions at the surface (i.e., evaporation and precipitation) with the Antilles Current assuming a secondary role.

ACOUSTICAL PROPERTIES

Using the observed temperature and salinity values and filling in intermediate depths where needed with computations at depths selected from the accepted temperature and salinity profiles, sound speed versus depth profiles were constructed based upon the equation of Wayne Wilson (1960). A composite of the resulting profiles for the stations in Area B is shown in Figure 11. Since the relation between temperature and sound speed is direct, the sound speed profiles bear a resemblance to the temperature versus depth composite down to about 1200 meters. The sound speed minimum occurs near this depth, below which an almost linear increase in sound speed due to pressure occurs. A large-scale plot of the finer sound speed structure of the upper 150 meters is shown in Figure 12 (A through E) arranged in the same sequence as the temperature and salinity plots. The same splitting of the profiles occurs which

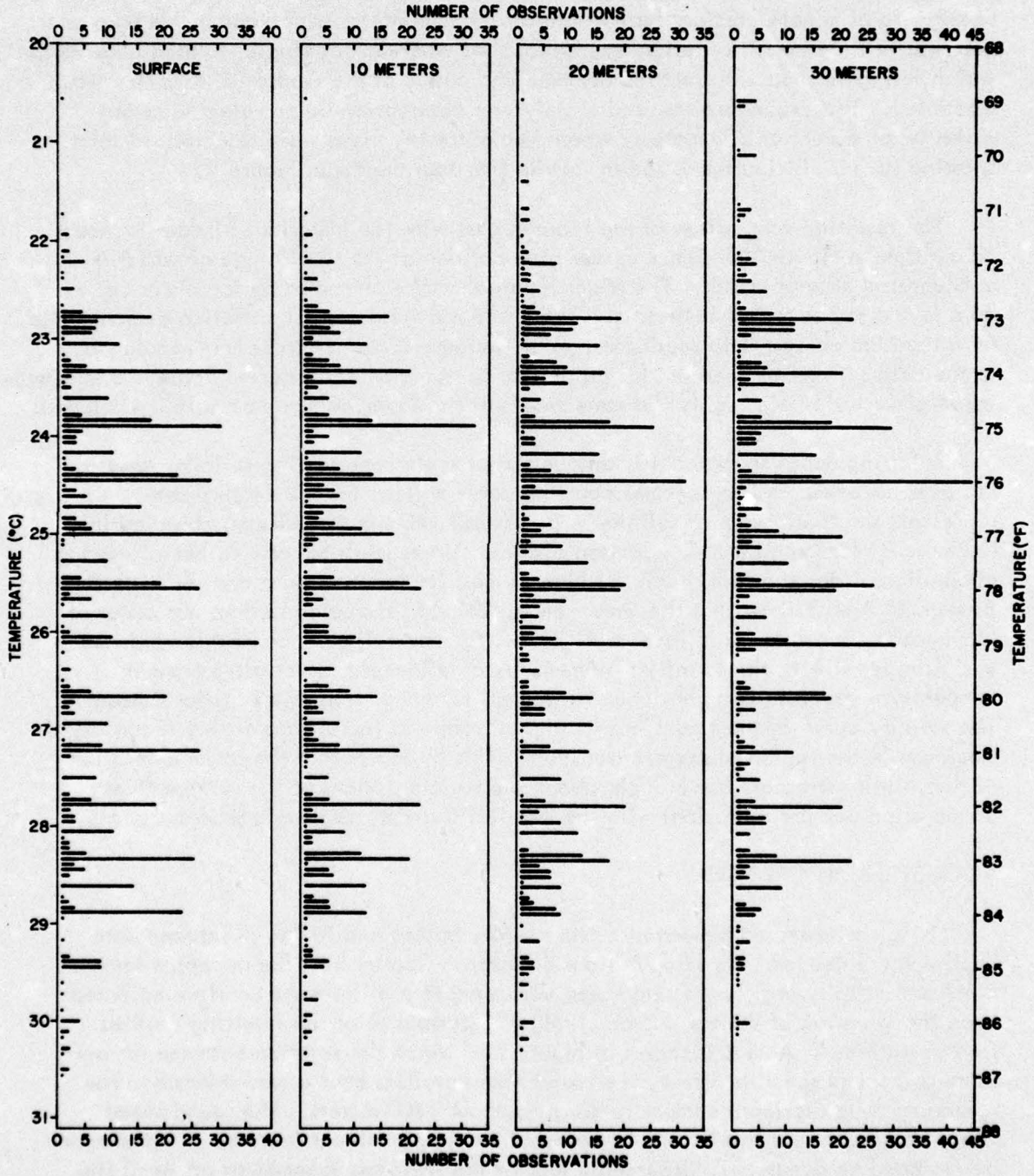

FIGURE 9 DISTRIBUTION OF BT TEMPERATURES AT SELECTED DEPTH

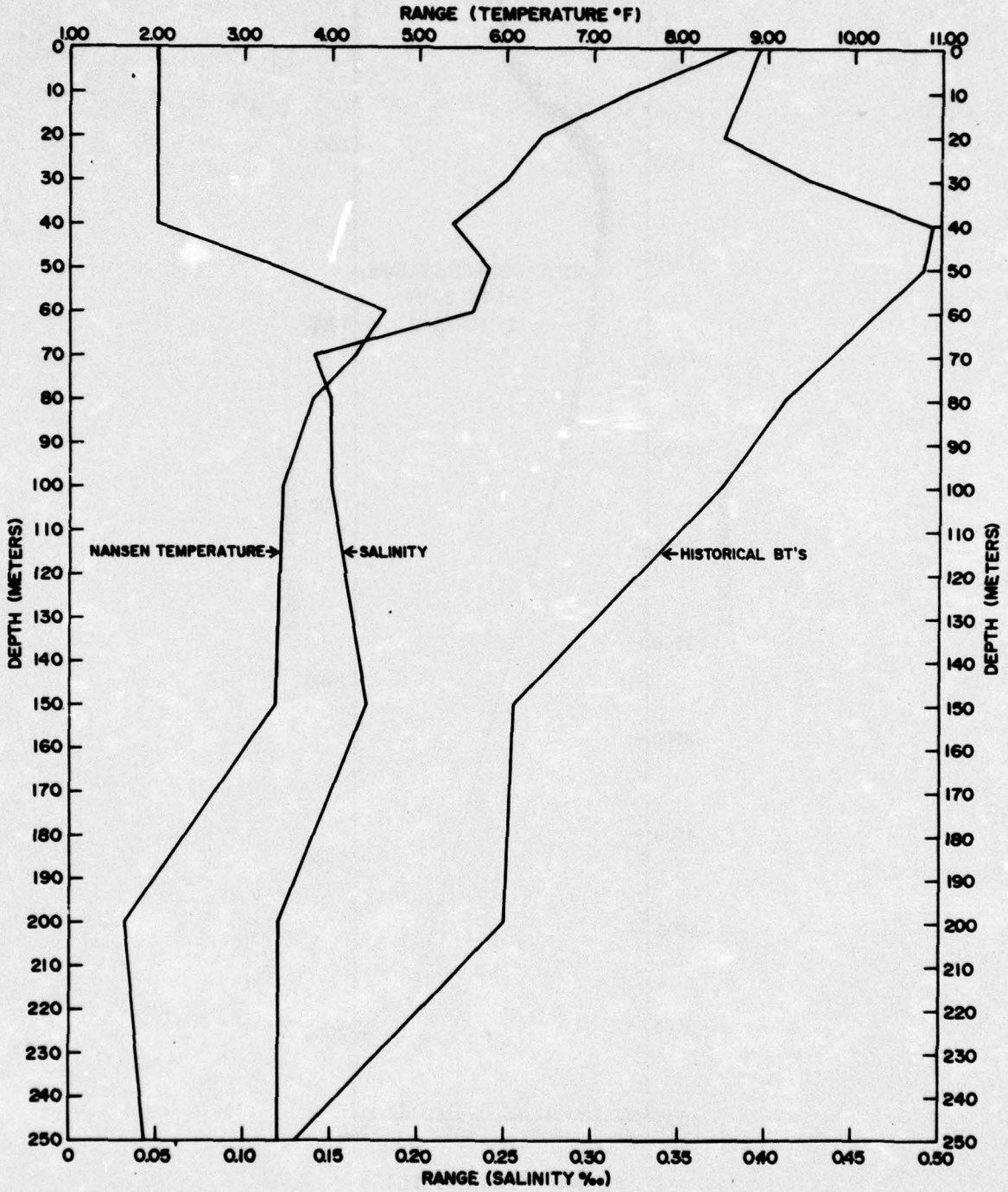

FIGURE 10 COMPARISON OF RANGE OF VARIATION OF NANSEN CAST

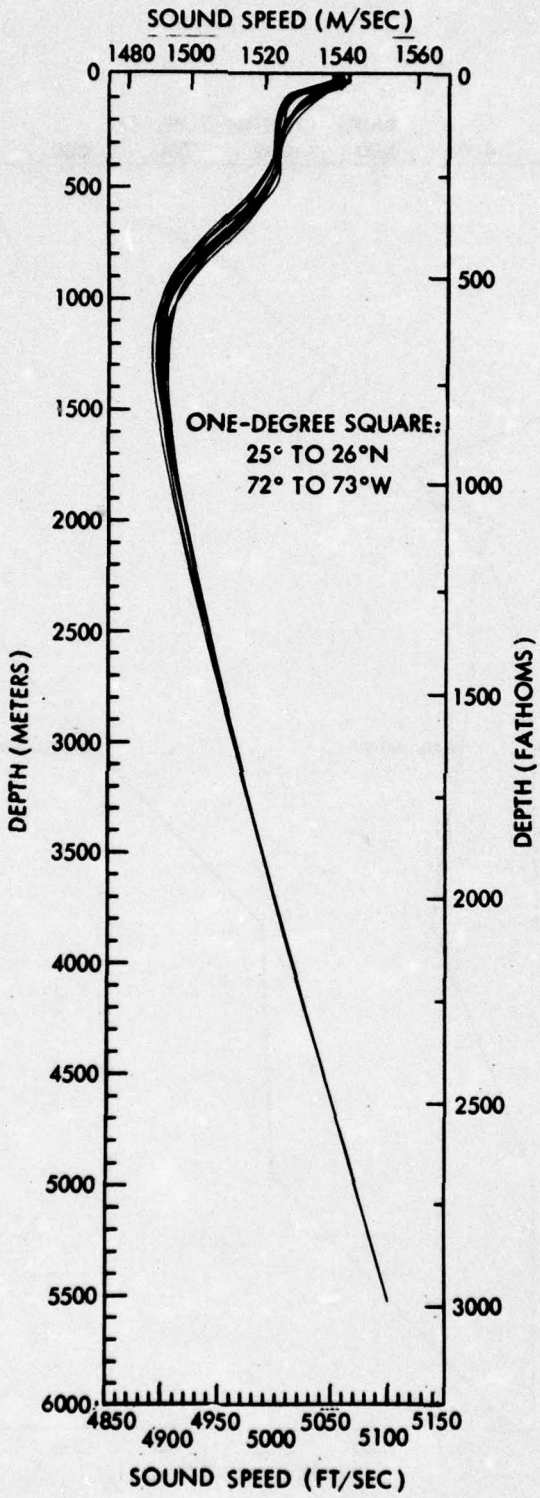

FIGURE 11 COMPOSITE SOUND SPEED GRAPH

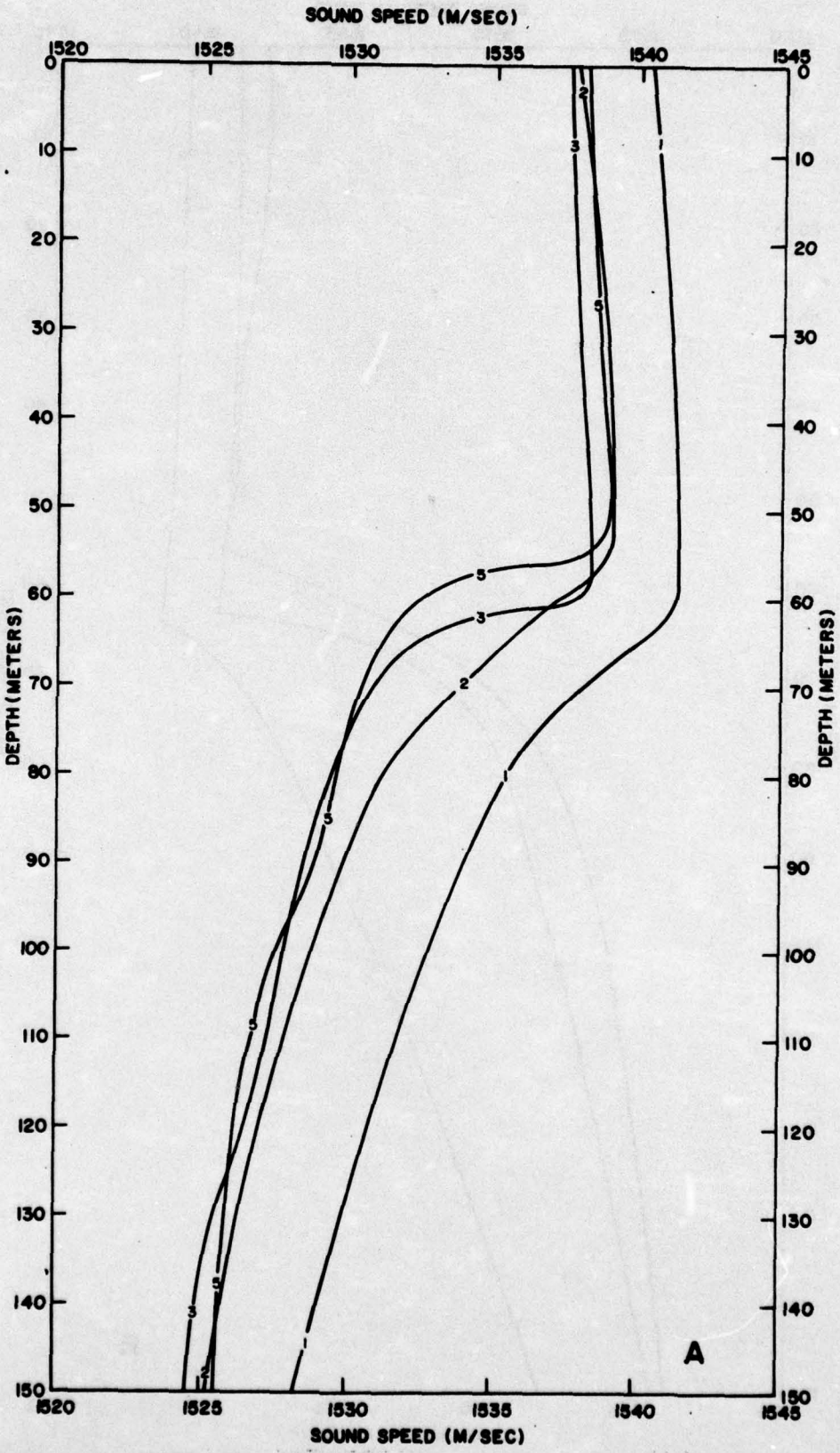

FIGURE 12A UPPER 150 METERS OF THE VERTICAL SOUND SPEED STRUCTURE

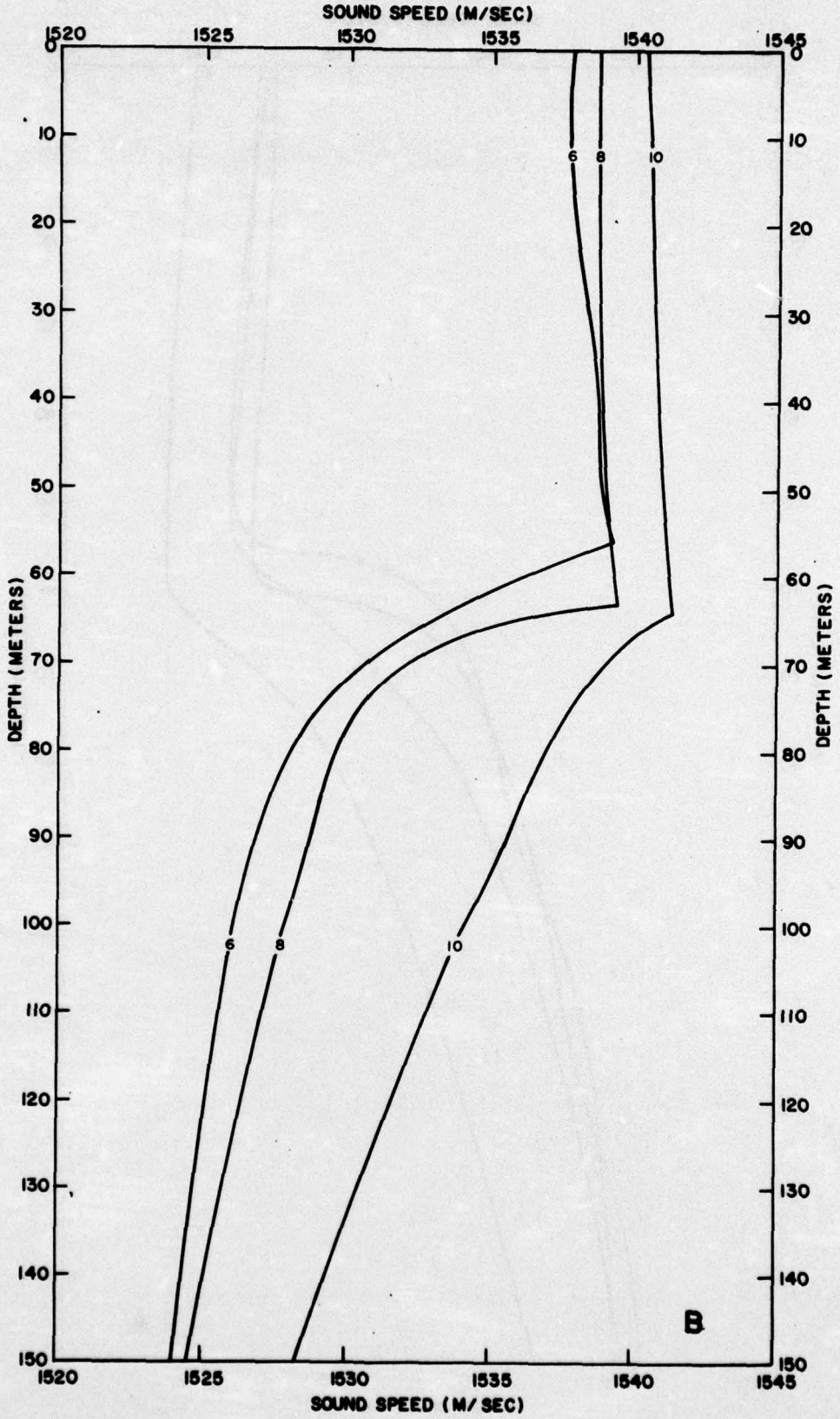

FIGURE 12B UPPER 150 METERS OF THE VERTICAL SOUND SPEED STRUCTURE

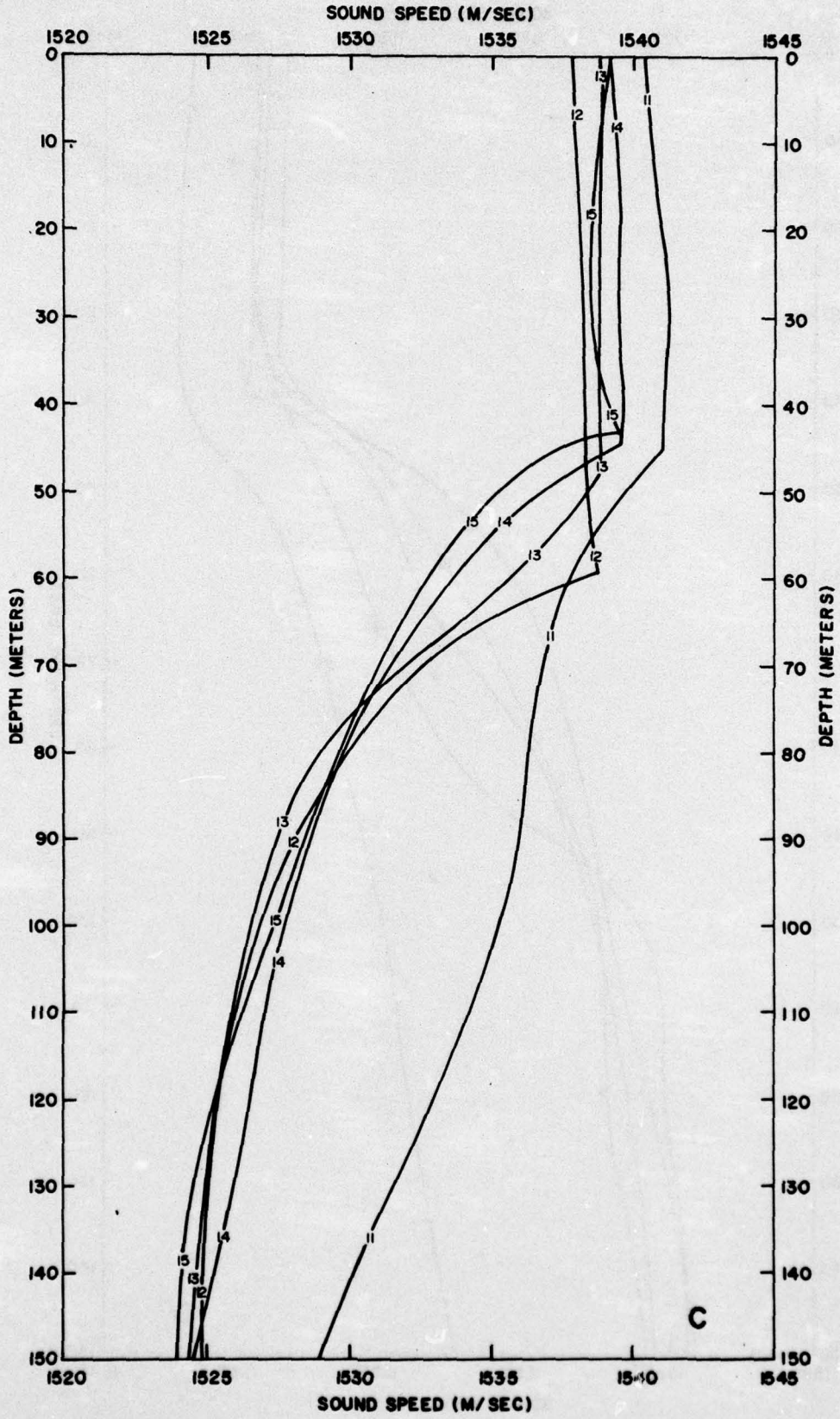

FIGURE 12C UPPER 150 METERS OF THE VERTICAL SOUND SPEED STRUCTURE

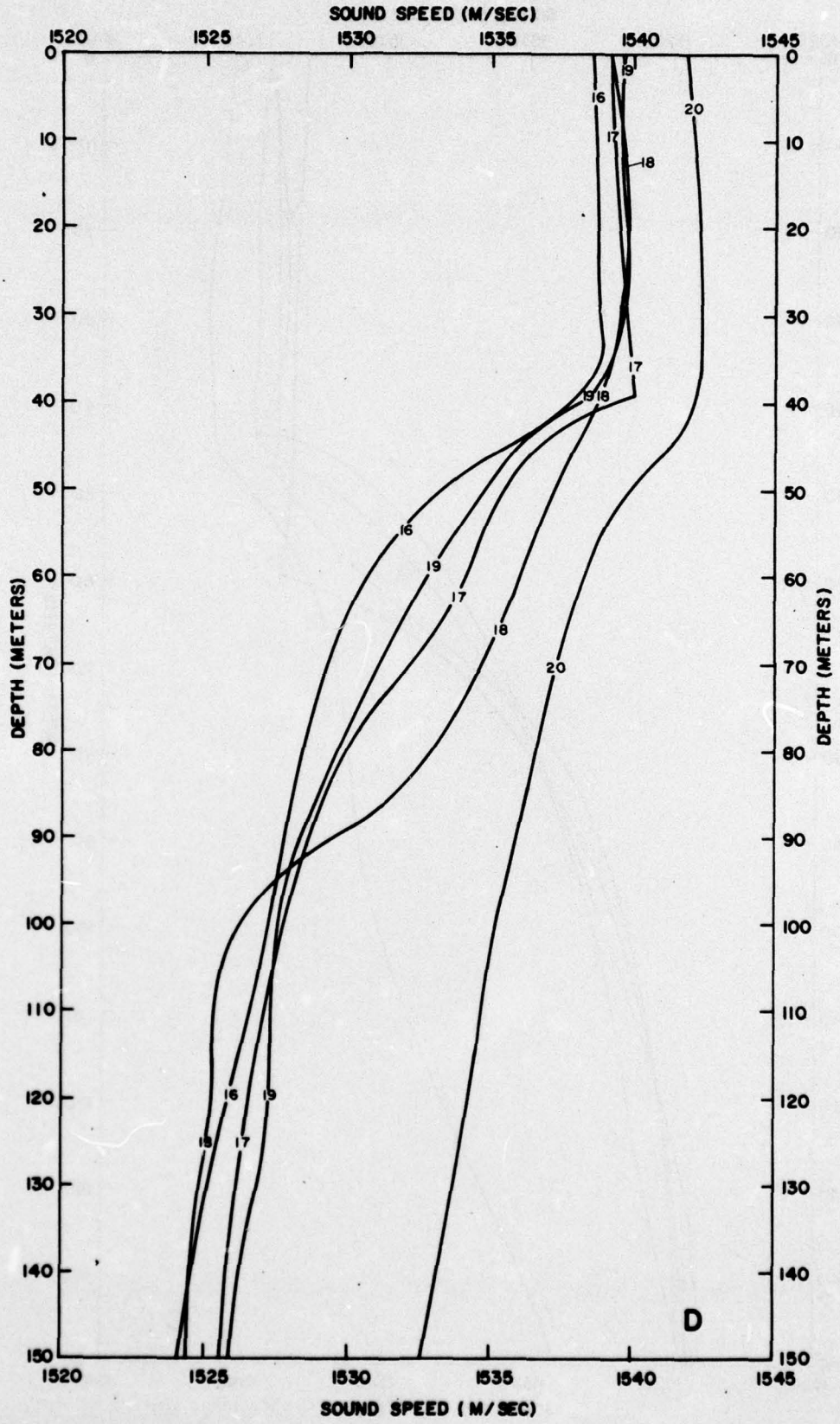

FIGURE 12D UPPER 150 METERS OF THE VERTICAL SOUND SPEED STRUCTURE

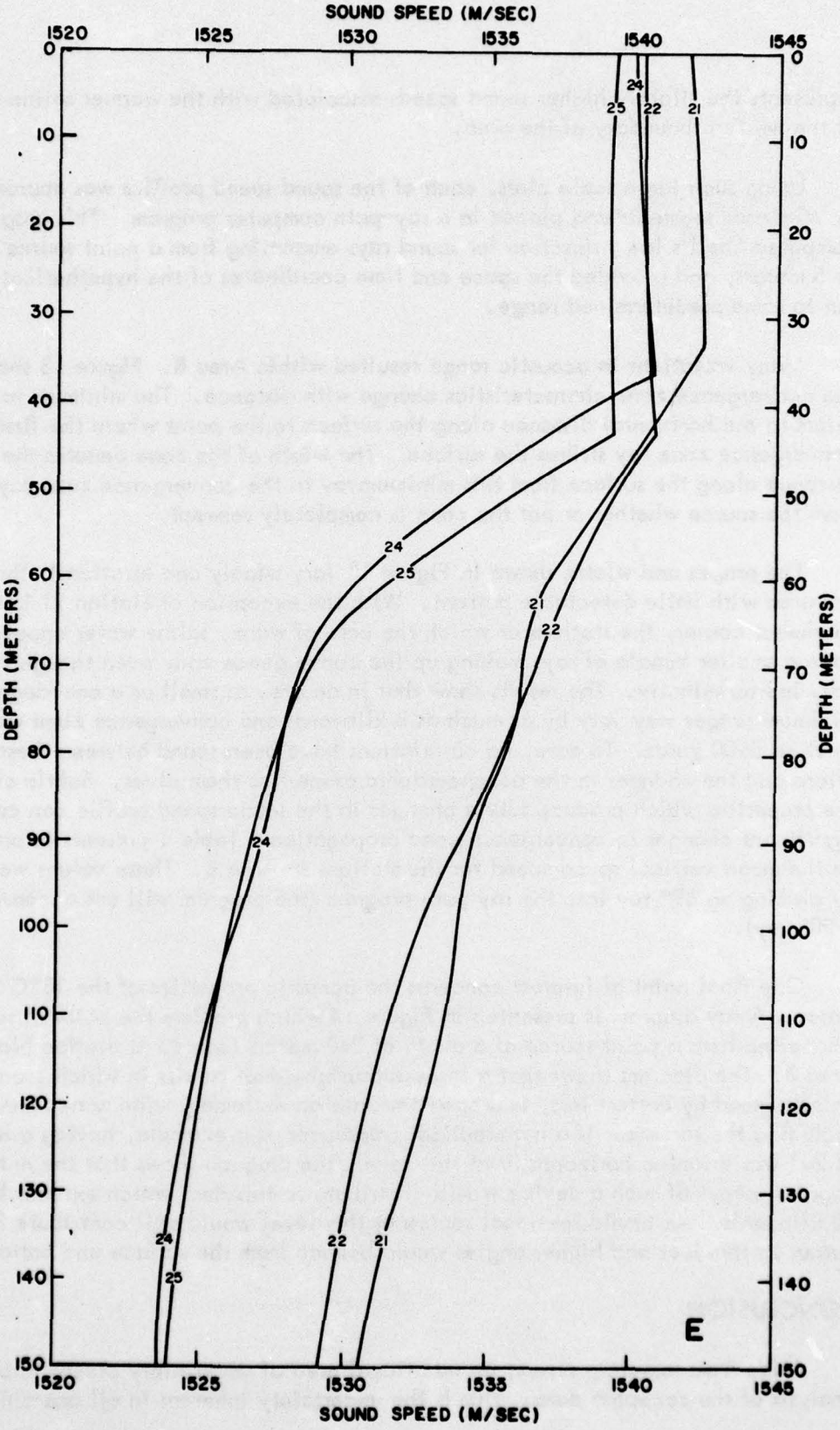

FIGURE 12E UPPER 150 METERS OF THE VERTICAL SOUND SPEED STRUCTURE

represents the slightly higher sound speeds associated with the warmer saline core of the western boundary of the area.

Using such large scale plots, each of the sound speed profiles was approximated by 40 linear segments and placed in a ray-path computer program. This program computed Snell's law refraction for sound rays emanating from a point source located at 5 meters, and provided the space and time coordinates of the hypothetical ray out to some predetermined range.

Many variations in acoustic range resulted within Area B. Figure 13 shows how the convergence zone characteristics change with distance. The minimum range refers to the horizontal distance along the surface to the point where the first refracted convergence zone ray strikes the surface. The width of the zone denotes the horizontal distance along the surface from this minimum ray to the convergence zone ray farthest from the source whether or not the zone is completely reswept.

The ranges and widths shown in Figure 13 vary widely and erratically throughout the area with little detectable pattern. With the exception of Station 21 in the southwest corner, the stations at which the core of warm, saline water appeared all have a smaller bundle of rays making up the convergence zone even though the widths vary indiscriminatly. The results show that in an area as small as a one-degree square, minimum ranges may vary by as much as 8 kiloyards and convergence zone widths by as much as 6900 yards. To date, no correlations have been found between these variations and the changes in the oceanographic properties themselves. Subtle changes in the properties which produce subtle changes in the sound speed profile can cause significant changes in convergence zone propagation. Table 1 presents information on the mean vertical sound speed for the stations in Area B. These values were computed by placing an 89° ray into the ray path program (the program will not accommodate a 90° ray).

One final point of interest concerns the acoustic properties of the 18°C Saragasso water. A ray diagram is presented in Figure 14 which predicts the paths of sound rays emanating from a point source at a depth of 240 meters located at Station No. 12 in Area B. The diagram shows that a large subsurface duct results in which sound, uninfluenced by bottom loss, is propagated into an extremely wide zone beneath and including the surface. If a hypothetical transducer, for example, having a beam width of 20° was oriented horizontally at this level, the diagram shows that the entire angular output of such a device would contribute to this duct which extends beyond 90 kiloyards. An omnidirectional source at this level would still contribute 20° of its output to the duct and higher angles would bounce from the surface and bottom.

CONCLUSION

Aside from sampling errors, an additional area of uncertainty creeps into the analysis of the accepted data. This is the uncertainty inherent in all one-ship surveys

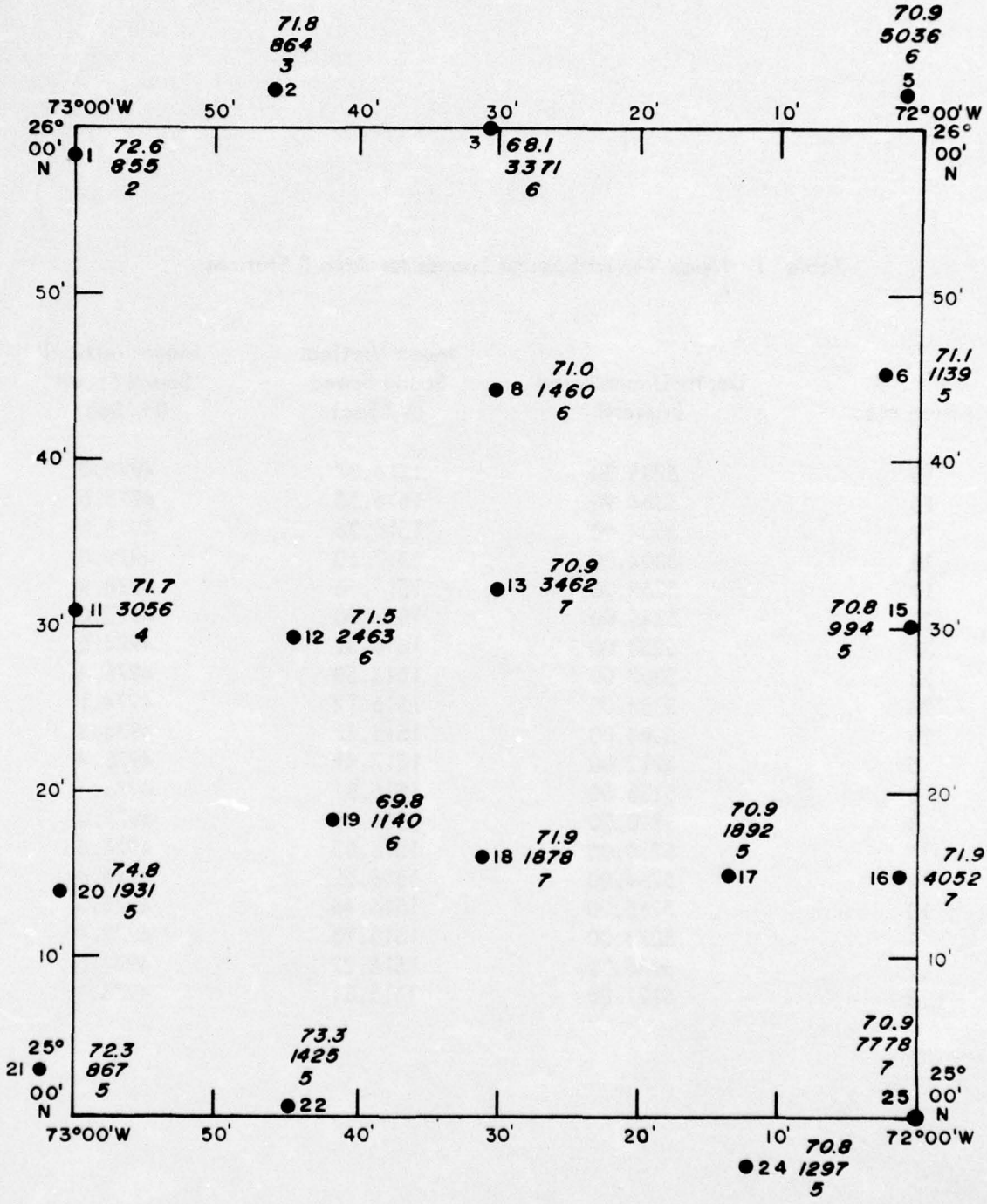

LEGEND

71.0 ← MINIMUM RANGE (KYDS)
1460 ← ZONE WIDTH (YDS)
6 ← NUMBER OF RAYS IN BUNDLE

FIGURE 13 CONVERGENCE ZONE VARIATIONS

Table 1 Mean Vertical Sound Speeds for Area B Stations

Station No.	Depth-Uncorrected (Meters)	Mean Vertical Sound Speed (M/Sec)	Mean Vertical Sound Speed (Ft/Sec)
15	5285.00	1516.37	4975.0
16	5304.90	1516.55	4975.5
17	5302.00	1516.76	4976.2
18	5304.00	1517.60	4979.0
19	5269.00	1516.96	4976.9
20	5245.00	1517.00	4977.0
21	5258.00	1516.32	4974.8
22	5307.00	1516.50	4975.4
24	5304.00	1516.12	4974.1
25	5304.00	1516.77	4976.3
5	5212.00	1517.41	4978.4
6	5238.00	1516.81	4976.4
8	5218.00	1516.99	4977.0
11	5210.00	1516.83	4976.5
12	5254.00	1516.52	4975.4
13	5265.00	1516.46	4975.3
1	5073.00	1515.78	4973.0
2	5066.00	1516.27	4974.6
3	5121.00	1515.81	4973.1

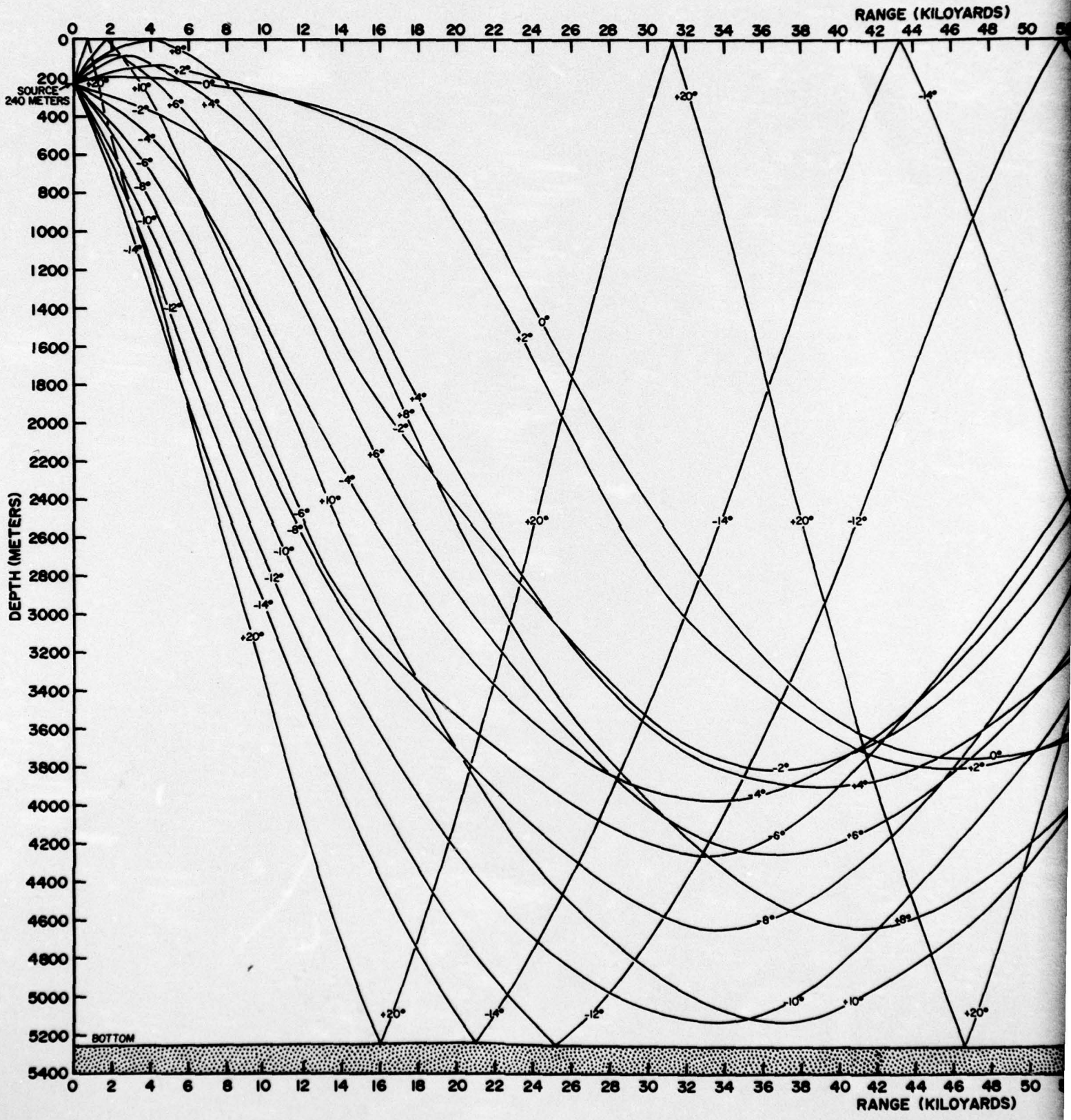

FIGURE 14 RAY DIAGRAM WITH SOUND SOURCE

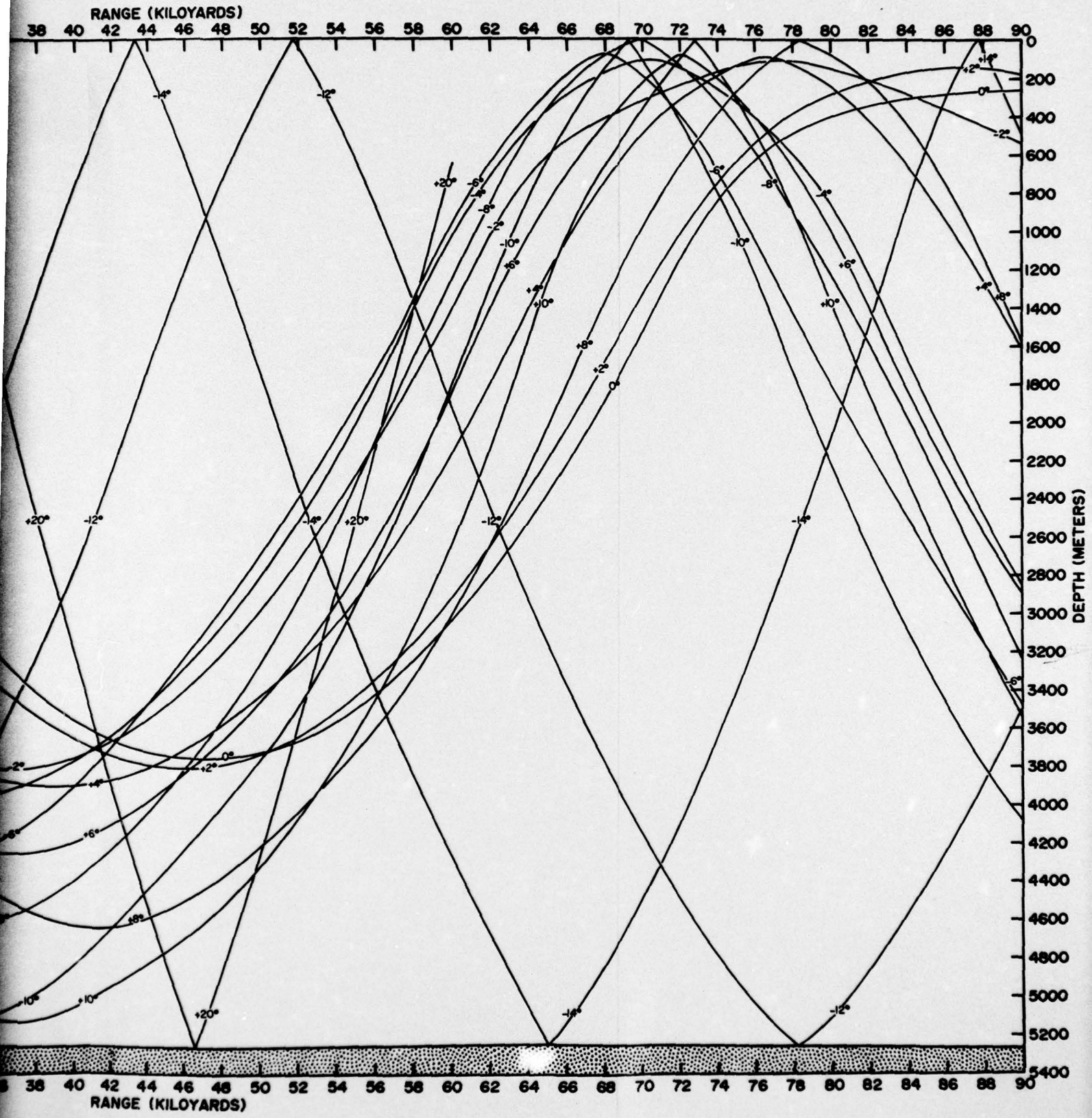

DIAGRAM WITH SOUND SOURCE AT DEPTH OF 18°C WATER

wherein the data collected represents a complex admixture of spatial and temporal variations. Time-series observations at several points taken simultaneously are needed to unscramble the time/space variations. Thus, the graphs and diagrams presented in this report must represent a somewhat confused picture of the true variation at any given instant. The contouring of the detached saline lens on the cross-sectional diagram C in Figure 8, for example, may very well have obscured a core on the western boundary in transit to the east, or any other complex motion. Or, the long saline layer contoured on diagram F of the same figure could possibly have been due to a small lens travelling in the direction of the ship and which was sampled 3 or 4 times at different locations and coutoured as a layer. The graphs and diagrams as they are presented in this study assume that the changes that take place are geographical in nature and represent a synoptic picture.

The acoustic analysis is susceptible to many errors beginning with the collection of the data and continuing through to the drawing of the final profiles. The Nansen cast method of obtaining acoustic information is helpful and informative, but it gives only computed values at discrete points. More reliable information could be elicited from measured values which are continuous with depth.

In a study in which acoustic information is to be extracted from temperature and salinity measurements, it is obvious that the acoustic results can be no more accurate than the temperature and salinity measurements upon which they are based. It is clear that the proper approach to the construction of sound speed profiles from Nansen cast data is not to begin the study with a construction of the sound speed profile, but rather to begin with the construction of the most accurate temperature and salinity profiles possible. From these profiles, a sound speed profile may be constructed based on points which are continuous with depth and thereby guaranteeing internal consistency between the oceanographic data and the resulting sound speed at every depth.

The ultimate data would be synoptic time-series measurement of all the oceanographic and acoustic properties at numerous locations within the area and continuous with depth. Recently, time sequence temperature measurements via thermistors were taken in conjunction with time sequence current observations as well as some Nansen casts in Area B. Results of these data should be available for study in the near future.

APPENDIX A COMMENTS ON THE DATA

Temperature

The measurements of temperature for this study are based upon the averaged values of paired reversing thermometers which are handled by fairly standardized procedures. When the readings from a given pair of thermometers differed by more than 0.07°C, the reading from the most reliable thermometer was accepted. Reliability considerations were based upon the previous history of the instrument in question. In this fashion, the temperature measurements are thought to be accurate to ±0.04°C.

Salinity

Measurements of salinity were made by an induction salinometer after the bottled samples were shipped to the Oceanographic Office. Utilizing standard techniques of determination, the accuracy of the data was considered correct to 0.01°/oo. In this study, no attempt was made to alter or reject any observed value of Nansen cast temperature or salinity in light of the foregoing judgements.

Bathythermographs

Of the 76 BT's reportedly taken on this cruise, 52 of them were converted into usable prints for this study. Of these, 46 were taken with one instrument. In an effort to compare and possibly calibrate readings, when a Nansen station was taken within the space and time of any of the BT's, the thermometric temperatures were plotted over the range of depths covered by the BT's, and the algebraic difference between the two values plotted. The resulting value was then compared graphically with the station data by referring the computed difference to the thermometric determination which is taken to be zero at all depths. After a series of such plots, as is shown in the typical one on Figure 15, it was noted that the one instrument used most on this cruise consistently showed temperatures which differed by some positive value up to 5°F after the BT had traveled beneath the mixed layer. Since it seemed unlikely that the BT should always differ by a higher temperature than the Nansen data, it was assumed that this instrument was making some systematic error. Other than being used in correlation with layer depth and temperatures within the layer, the BT's from the PREVAIL cruise were rejected for this study. The 6 remaining BT's taken with another instrument were not used since no Nansen data were taken during the 2 days when it was employed.

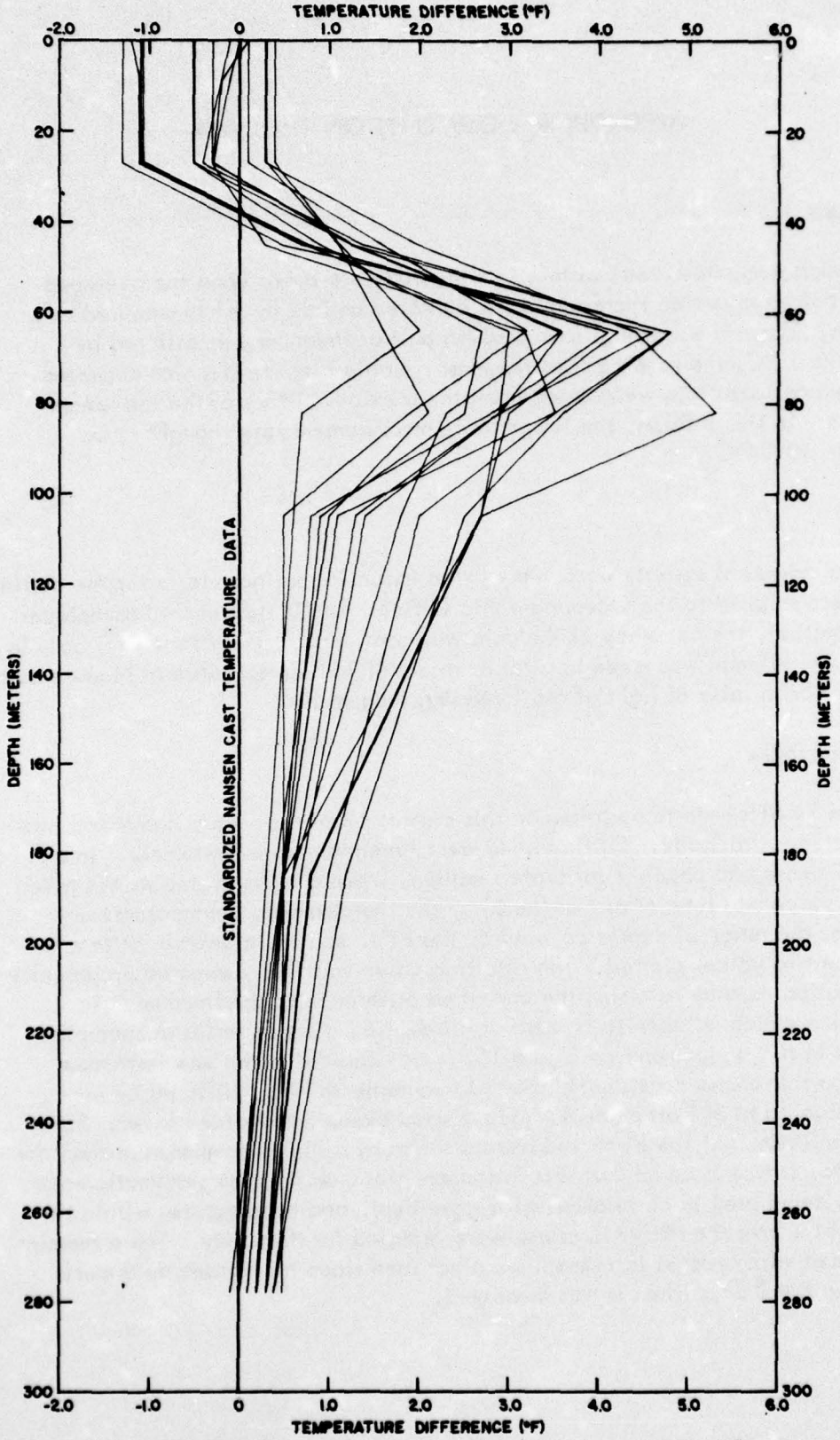

FIGURE 15 DIFFERENCE BETWEEN BT AND NANSEN TEMPERATURES USING THE NANSEN DATA AS A REFERENCE

REFERENCES

Defant, Albert, Physical Oceanography, Vol. I, New York, Pergamon Press Ltd., pp. 165-173, 1961.

Officer, Charles B., et al., Acoustic and Geophysical Survey of Bottom and Subbottom Reflections Area B, Parts I-III, Norwood, New Jersey, Alpine Geophysical Associates, Inc., 17 February 1964, Unpublished.

Parr, Albert Eide, "A Contribution to the Hydrography of the Caribbean and Cayman Seas", Collected Reprints Woods Hole Oceanographic Institution, Part I, No. 125, Woods Hole, Massachusetts, Woods Hole Oceanographic Institution, p. 110, 1937.

Schott, Gerhard, Geographie Des Atlantischen Ozeans, Hamburg, C. Boysen, pp. 263-267, 1947.

Schroeder, Elizabeth and Stommel, Henry, "Climatic Stability of Eighteen Degree Water at Bermuda", Journal of Geophysical Research, Vol. 64, No. 3, pp. 363-366, 1959.

Sverdrup, H. V., The Oceans, Englewood Cliffs, New Jersey, Prentice-Hall, Inc., pp. 605-761, 1957.

U. S. Naval Oceanographic Office, Tables of Sound Speed in Sea Water, NAVOCEANO SP-58, Washington, D. C. p. 47, 1962.

Wilson, Wayne D., "Speed of Sound in Sea Water as a Function of Temperature, Pressure, and Salinity", Journal of the Acoustical Society of America, Vol. 32, No. 6, pp. 641-644, June 1960.

Worthington, L. V., "The 18° Water in the Sargasso Sea", Deep Sea Research, Vol. 5, London, Pergamon Press Ltd., pp. 297-305, 1959.

Wust, Georg, "Florida-und Antillenstrom", Berlin Universitat Institut Fur Meereskunde, Veroffentlichungen neuefolge Reihe A, No. 11-17, Berlin, E. S. Mittler & Son, p. 48, 1924.

- - - "Der Golfstrom", Zeitschrift Der Gesellschaft für Erdkunde Zu Berlin, p. 59, 1930.